



Contents lists available at ScienceDirect

European Journal of Control

journal homepage: www.elsevier.com/locate/ejcon

Event-triggered sliding mode based consensus tracking in second order heterogeneous nonlinear multi-agent systems^{☆☆}

Rajiv Kumar Mishra^{a,b}, Abhinav Sinha^{c,*}

^aSchool of Electronics Engineering, Kalinga Institute of Industrial Technology, Bhubaneswar, India

^bDepartment of Computer Science, School of Computing, Tokyo Institute of Technology, Japan

^cIndian Institute of Technology, Bombay (Mumbai), India

ARTICLE INFO

Article history:

Received 27 August 2017

Revised 1 September 2018

Accepted 17 October 2018

Available online xxx

Recommended by Dr X Chen

Keywords:

Heterogeneous second order multi-agent systems (MAS)

Event-triggered leader following Tracking control

Event-triggered sliding modes

Inter event execution time

Inverse sine hyperbolic reaching law

Nonlinear gain

Consensus

Formation keeping

ABSTRACT

This work targets the problem of leader following consensus in heterogeneous multi-agent systems described by second order nonlinear dynamics. The controller proposed in the study is an event-based sliding mode controller. Synthesis of the controller has been partitioned into two parts– a finite time consensus problem and an event-based control mechanism. In the first part, the leader following heterogeneous multi-agents of second order having inherent nonlinear dynamics have been addressed and a novel sliding mode reaching law based on inverse sine hyperbolic function has been designed to drive the agents towards consensus. In the second part, an event-based implementation of the control law has been incorporated to minimize computational load on the computational device equipped with the agents and reduce energy expenditure. The triggering rule proposed in this work is dynamic and taking samples respecting this rule ascertains that the desired closed-loop performance of the system is not compromised while exhibiting robustness and high efficacy. The advantage of using such a scheme, i.e., an event-based sliding mode controller is rooted in the robustness capabilities of sliding mode controller and reducing computational expenses via event-based mechanisms. Numerical simulations and mathematical foundations confirm the effectuality of the controller proposed in this study.

© 2018 European Control Association. Published by Elsevier Ltd. All rights reserved.

1. Introduction

1.1. Overview

Recently, the distributed cooperative control of Multi-Agent Systems (MAS) has drawn attention of diverse research community. The main application domains of MAS are ambient intelligence, grid computing, electronic business, the semantic web, bioinformatics and computational biology, monitoring and control, resource management, education, space, military and manufacturing applications, and so on. Many researchers have applied agent technology to industrial applications such as manufacturing enterprise integration, supply chain management, manufacturing planning, scheduling and control, holonic manufacturing systems, etc. A small perturbation in a single agent can adversely affect the entire

interconnected network of MAS. Contrary to a single autonomous agent, MAS provides higher degree of redundancy and improvement on operational efficiency. Moreover, MAS exploits the advantage of having distributed sensing and actuation [42–44]. A particularly challenging problem in this field is commonly referred to as consensus. A consensus algorithm or protocol is an interaction rule that specifies the information exchange between an agent and all of its neighbors on the network [33]. The objective of MAS consensus is to devise a network distributed control algorithm such that all agents reach an agreement on certain quantities of interest via local interaction. A group of autonomous agents should possess the ability to interact amongst themselves or with their environments and are required to accomplish some specified task together as a single entity to reach a common goal. Agents could be homogeneous, i.e., their dynamics are identical, or heterogeneous, i.e., dynamics of each agent is different. Heterogeneous agents are of relatively higher practical significance than their homogeneous counterparts. Another interesting and challenging problem in this area is referred to as formation control of MAS. The objective of formation control is to move the agents cohesively in a specified geometrical pattern to perform a cooperative task. The obvious advantages of having achieved formation of MAS are high probability

[☆] ORCID: 0000-0001-6419-2353

^{☆☆} ORCID: 0000-0002-4322-3349

* Corresponding author.

E-mail addresses: mishra@sc.dis.titech.ac.jp (R.K. Mishra), sinha.abhinav@iitb.ac.in (A. Sinha).

<https://doi.org/10.1016/j.ejcon.2018.10.003>

0947-3580/© 2018 European Control Association. Published by Elsevier Ltd. All rights reserved.

of success, cost and energy efficiency, robustness, accuracy and increased feasibility.

1.2. Brief survey

The intriguing animal group behaviors and observations in nature such as schooling of fish, swarming of bacteria, flocking of birds, etc. have led to the development of protocols for cooperative behavior of MAS. Reynolds [39] simulated the first computer model to study flocking behavior of multi-agents. Su and Huang [52,61] studied consensus problem of the leader-follower MAS having linear dynamics and switching topology. Li et al. [26] proposed an adaptive consensus protocol for homogeneous MAS with each agent having different uncertainties. Beard and Atkins [38] studied the asymptotic consensus problem for MAS having single integrator dynamics. Dong and Huang [14] investigated the asymptotic consensus problem for MAS having double integrator dynamics. Ren and Beard [37] proposed that asymptotic consensus can be obtained in MAS having first order dynamics only if the network contains a directed spanning tree. Yu et al. [65] proposed that the consensus in a higher order MAS can be obtained only if the Laplacian matrix has all non-zero eigenvalues lying in the stable consensus regions. Khoo et al. [23] observed finite time consensus of leader-follower second order MAS with an application of terminal sliding mode control. A stationary average consensus protocol for higher order homogeneous MAS based on state and output feedback has been proposed in [40]. Peymani et al. [34] studied H_∞ consensus problem of heterogeneous MAS. In many practical applications, the individual autonomous agents of MAS might have different dynamics. It has also been observed that even homogeneous agents inevitably drift towards heterogeneity over time. Wang et al. [56] proposed that heterogeneous multi-robot systems with agent having different features are more applicable as opposed to their homogeneous counterparts. Zheng et al. [68] studied the linear and saturated consensus algorithm for MAS with heterogeneous agent having first order and second order integrator dynamics. Most of the MAS model studied in literature consider a first order or second order integrator dynamics of agents, however in practice, individual autonomous agents may have some inherent nonlinear dynamics. Yu et al. [64] investigated the leaderless consensus problem of a second order MAS with inherent nonlinear dynamics under fixed network topology. Zheng and Wang [67] studied distributed consensus problem of a heterogeneous MAS with fixed and switching topologies. Zhou et al. [69] proposed finite time consensus protocol for higher order heterogeneous multi-agent systems based on state and output feedback. Wen et al. [59] investigated consensus of MAS with higher order Lipschitz-type nonlinear dynamics under switching topology. Wang et al. [57] discussed the formation control problem of flying of multiple unmanned air vehicle (UAV) navigating through an obstacle-laden environment. Zhao & Tiauw [58] proposed multiplexed model predictive control for formation control of multiple UAV which resulted in collision and obstacle avoidance. Other research works on UAVs and formation keeping have been discussed in [17,21,27,47,60] to mention a few.

With the advancement of embedded systems, almost all the controllers are realized in sampled data approach owing to its easy implementation properties. Therefore, the practical approach to solve leader-follower consensus problem is to use sampled data control, especially in bandwidth and energy constrained environments. The traditional sampled data control system considers periodic update of the controllers even after achieving control objective. The measurements are sampled and control is updated periodically even if the system may tolerate fluctuations in some allowable range. This results in wastage of significant computational and communication resources. An efficient way

to reduce communication and computational burden is to use event-triggering scheme. The samples are obtained only when an event is triggered. The objective of the event-triggering scheme is to sample and update controller only when the local measurement error crosses a predefined threshold while ensuring satisfactory closed-loop performance of the system. An event-triggering scheme for linear quadratic control has been proposed in [3], in which the system model was linear and performance was measured by an average quadratic cost. If the Euclidean norm of the error between the state and a state prediction exceeded a threshold, then event was triggered to update the controller. An event-driven consensus problem of linear MAS under fixed topology has been investigated in [70]. The problem of event-triggered leader-follower consensus for a second order MAS with a fixed topology as well as a switching topology has been studied in [25]. Guo and Dimarogonas [20] proposed event-triggered nonlinear consensus protocol for homogeneous MAS having single integrator dynamics. Garcia et al. [16] investigated event-based consensus of leader-follower heterogeneous MAS with linear dynamics. In [3], the triggering rule is static and in [16], the triggering rule is time varying but not dynamic. It should be noted that the communication among follower agents in [25,40,69,70] are continuous, eventually leading to significant wastage of available resources, as well as the consensus protocol is also conservative. In this work, we have addressed consensus problem of consensus tracking in a second order leader-follower heterogeneous MAS having inherent nonlinear dynamics under directed graph topology using event-triggered sliding mode control.

1.3. Contributions

The main contributions of this work are summarized below.

1. The finite time consensus problem of a second order heterogeneous multi-agent system with inherent nonlinear dynamics has been considered here. Dynamics of the agents considered in this work are more general as opposed to those appearing in the literature of MAS. When the uncertain functions are zero, the problem reduces to those of integrator dynamics, and when the functions are linear, the problem shapes into that of a linear one.
2. The proposed controller is an event-based controller designed on the paradigms of sliding mode. An inverse sine hyperbolic based novel reaching law has been put forward to cope up with the scenario. Due to odd and monotonous nature of this function, the gain of this controller is adaptive and nonlinear. When the trajectories are far away from the sliding manifold, the gain is larger in magnitude as compared to when trajectories are in vicinity of the manifold. This shortens the reaching phase and the control signal is smooth and fast.
3. The proposed control strategy ensures robust consensus tracking even in the presence of bounded disturbances and matched uncertainties.
4. The event-triggering rule used in this work is novel and dynamic in nature as opposed to many time varying triggering used in literature such as in [16], depending not only on the local topological error variables but also on non-topological errors. The inter execution time, i.e., the time interval between two consecutive controller updates is bounded below by a finite positive quantity, thereby ensuring no *Zeno* behavior.
5. Formation control of MAS has also been demonstrated to further aid the proposition.

1.4. Organization of the paper

The remainder of this work is organized as follows. Section 2 introduces preliminary concepts related to spectral graph theory

and event-based sliding mode control. Model description of the heterogeneous second order MAS with inherent nonlinear dynamics has been described in section 3. Controller synthesis has been described in section 4. Section 5 presents the simulation results and efficacy of the proposed control and finally, we conclude the paper in section 6. Recommendations for future work have been provided in section 7.

2. Preliminaries

2.1. Spectral graph theory for multi agent systems

A directed graph, also known as digraph [10] is represented here by $\mathcal{G} = (\mathcal{V}, \mathcal{E}, \mathcal{A})$. \mathcal{V} is the nonempty set that contains finite number of vertices or nodes [9,13] such that $\mathcal{V} = \{1, 2, \dots, N\}$. \mathcal{E} denote edges that are directed and are represented as $\mathcal{E} = \{(i, j) \mid \forall i, j \in \mathcal{V} \text{ \& } i \neq j\}$. \mathcal{A} is the weighted adjacency matrix such that $\mathcal{A} = a(i, j) \in \mathbb{R}^{N \times N}$.

The existence of an edge (i, j) is possible if and only if the vertex i receives the information supplied by the vertex j , i.e., $(i, j) \in \mathcal{E}$. Hence, i and j are referred to as neighbours. Let us consider a set \mathcal{N}_i that contains labels of vertices that are neighbour of the vertex i . For the adjacency matrix \mathcal{A} , $a(i, j) \in \mathbb{R}^+ \cup \{0\}$. If $(i, j) \in \mathcal{E} \Rightarrow a(i, j) > 0$. If $(i, j) \notin \mathcal{E}$ or $i = j \Rightarrow a(i, j) = 0$.

The Laplacian matrix \mathcal{L} [10,11,19] lies at the heart of the consensus problem and is given by $\mathcal{L} = \mathcal{D} - \mathcal{A}$ where \mathcal{D} is a diagonal matrix, i.e., $\mathcal{D} = \text{diag}(d_1, d_2, \dots, d_n)$ whose entries are $d_i = \sum_{j=1}^n a(i, j)$. \mathcal{D} is known as degree matrix in the notions of graph theory. A directed path from vertex j to vertex i defines a sequence comprising of edges $(i, i_1), (i_1, i_2), \dots, (i_l, j)$ with distinct vertices $i_k \in \mathcal{V}$, $k = 1, 2, 3, \dots, l$. \mathcal{B} is also a diagonal matrix with entries 1 or 0 and is commonly referred as incidence matrix. If there exists an edge between leader agent and any other agent, the entry is 1 and 0 otherwise. Furthermore, it can be inferred that the path between two distinct vertices is not uniquely determined. However, if a distinct node in \mathcal{V} contains directed path to every other distinct node in \mathcal{V} , then the directed graph \mathcal{G} is said to have a spanning tree.

Physically, each agent in the multi agent system is represented by a vertex or node and the line of communication between any two agents is represented as a directed edge. The relationship between \mathcal{G} and \mathcal{V} establishes the following lemmas:

Lemma 2.1. Consider a directed graph \mathcal{G} and its Laplacian matrix \mathcal{L} . The set of eigenvalues of \mathcal{L} contains at least one zero eigenvalue. Other nonzero eigenvalues of \mathcal{L} have positive real parts. \mathcal{L} has a simple zero eigenvalue only when \mathcal{G} has a spanning tree. Also, \mathcal{G} is said to be balanced if the following criterion is met:

$$\mathcal{L}\mathbf{1}_N = \mathbf{1}_N^T \mathcal{L} = \mathbf{0}_N. \quad (1)$$

Here $\mathbf{1}_N$ denotes a column vector of all 1s, i.e., $[1, 1, \dots, 1]^T$ and $\mathbf{0}_N$ denotes a column vector of all 0s, i.e., $[0, 0, \dots, 0]^T$. Both $\mathbf{1}_N$ and $\mathbf{0}_N \in \mathbb{R}^N$. The elements of \mathcal{L} are denoted as $l(i, j)$ such that $l(i, j) \in \mathbb{R}^{N \times N}$.

Lemma 2.2. The matrix $\mathcal{L} + \mathcal{B}$ has full rank when \mathcal{G} has a spanning tree with leader as the root. This implies non singularity of $\mathcal{L} + \mathcal{B}$.

Proofs of the lemmas described above can be found in [11] and thus, are safely omitted here.

2.2. Event-triggered Sliding Mode Control

Sliding Mode Control (SMC) [55,63] is known for its inherent robustness. The switching nature of the control is used to nullify bounded disturbances and matched uncertainties. The switching happens about a surface (hyperplane) in state space known as sliding surface (hyperplane). The control forces the system monotonically towards the sliding surface and this phase is regarded as

reaching phase. When the system reaches the sliding surface it remains there for all future time, thereby ensuring that the system dynamics remain independent of bounded disturbances and matched uncertainties. The controller has a reaching phase (trajectories in phase plane emanate and move towards the switching surface) and a sliding phase (trajectories in the phase plane that reach the switching surface try to remain there).

2.2.1. Reaching phase

Let the hyperplane discussed be given as $\sigma(x)$. In order to drive state trajectories onto this manifold, a proper discontinuous control effort $u(t, x)$ needs to be synthesized that satisfies the inequality

$$\sigma^T(x) \dot{\sigma}(x) \leq -\eta \|\sigma(x)\|, \quad (2)$$

with η being positive and is called the reachability constant.

$$\therefore \dot{\sigma}(x) = \frac{\partial \sigma}{\partial x} \dot{x} = \frac{\partial \sigma}{\partial x} f(t, x, u) \quad (3)$$

$$\therefore \sigma^T(x) \frac{\partial \sigma}{\partial x} f(t, x, u) \leq -\eta \|\sigma(x)\|. \quad (4)$$

The hyperplane or the surface variable is usually a function of error variables. In traditional sliding mode control theory, the surface variable takes the form

$$\sigma(x) = \left(\frac{d}{dt} + h \right)^{n-1} e,$$

where h is the scalar coefficient weight, $n-1$ is the relative degree between the output and the input of the system, and e is the relevant error variable.

2.2.2. Sliding phase

The motion of state trajectories confined on the switching manifold is known as *sliding*. A sliding mode is said to exist if the state velocity vectors are directed towards the manifold in its neighbourhood [63,66]. Under this circumstance, the manifold is called attractive [66], i.e., trajectories starting on it remain there for all future time and trajectories starting outside it tends to it in an asymptotic manner.

$$\therefore \dot{\sigma}(x) = \frac{\partial \sigma}{\partial x} f(t, x, u)$$

Hence, in sliding motion

$$\frac{\partial \sigma}{\partial x} f(t, x, u) = 0. \quad (5)$$

Then $u = u_{eq}$ (say) be a solution and is generally referred to as the equivalent control. This u_{eq} is not the actual control applied to the system but can be thought of as a control that must be applied on an average to maintain sliding motion. It is mainly used for analysis of sliding motion [62].

In practice, individual autonomous agents in MAS are often equipped with small digital microcontrollers to reduce the cost. These microcontrollers have limited computing and communication capabilities. According to traditional sampled data control systems theory, samples of measured output are obtained in a periodic fashion with a fixed sampling rate. In addition to this, a zero order hold operator is needed to maintain the control input signal constant between successive sample instants. This sampling technique is known as periodic sampling and is generally done along the time axis, also known as *Riemann* sampling [6]. An alternative and more efficient way to obtain samples along the dependent variable axis (vertical axis), known as *Lebesgue* sampling [6]. Under this technique, sampling interval is no longer periodic and samples are obtained only when a *noticeable change*, also referred to as an *event*, occurs. As a result, the controller does not need to update itself periodically, but a hold type operator is still

needed to maintain the value constant between successive sample instants. The continuous sampling and transmission, along with the occupancy of central processing unit to perform computations when the signal is constant (not changing too frequently) lead to significant waste of available resources. The optimum utilization of communication, computing and energy expenses is a concern in various applications with increasing number of systems getting networked. One mitigation strategy adopted is event-based control wherein control is applied only when the system calls for it depending upon some *event*. Event-based sampling is a trade-off between performance and sampling frequency. More formal presentation and earlier contributions on event-based control are presented in Refs. [1,2,4,5,8,24,29,30,41,48,49,53,54].

As a consequence of combining event-based strategies with sliding mode control, the robustness of the system has been retained while maintaining lower computational expense. However, the system trajectories tend to move away from the sliding manifold till the control is updated again but remain bounded within a band. Detailed discussion has been carried out in later sections.

3. Dynamics of multi-agent systems

Consider a heterogeneous second order multi agent system consisting of a virtual leader and a finite number of followers interconnected in a well defined directed topology. Under such interconnection, information of the leader's states is not available globally. However, local information is obtained through communication among follower agents. The governing dynamics of the multi agent system (MAS) is described by nonlinear differential equations as

$$\begin{aligned}\dot{x}_0 &= v_0, \\ \dot{v}_0 &= f(x_0, v_0) + u_0 + \zeta_0,\end{aligned}\quad (6)$$

and

$$\begin{aligned}\dot{x}_i &= v_i, \\ \dot{v}_i &= f_i(x_i, v_i) + u_i + \zeta_i,\end{aligned}\quad (7)$$

where $f_i(\cdot, \cdot)$ denotes general nonlinear dynamics of each agent in the multi-agent systems which is assumed to be known and is taken to be continuous in t . It should be noted that the function may represent a wide class of systems such as discontinuous, not fully linearizable, etc. x_0 and v_0 are the position and velocity of the virtual leader respectively and u_0 is the associated control with the leader agent such that $\|u_0\|_\infty \leq \Delta$ for some $\Delta \in \mathbb{R}^+$. This makes quite a practical case when upper limits on hardware constraints are known but the information on real time control effort is not concrete. Quite similarly x_i and v_i are the corresponding states of i^{th} follower and the associated control with each follower agents is u_i . ζ_0 and ζ_i are exogenous disturbances that may affect the system. It should be noted that $i \in \{1, 2, \dots, N\}$ and N is the total number of agents. In the synthesis of control, we shall assume that full state is available for feedback and sensors for measurement of states are noise free.

Remark 1. The dynamics of each agent is affected by the interconnection among agents as well as the presence of inherent nonlinearity in each agent.

Remark 2. For $f(\cdot, \cdot) = 0$, the problem reduces to the widely studied problem of double integrator system, and thus, control methodology of such systems can be extracted from the results presented in this study.

Remark 3. For the sake of simplicity, the foregoing discussion in this work takes into account the dimension as one, i.e., $x_i, v_i \in \mathbb{R}^1$. However, the same can be extended to higher dimensions by invoking Kronecker products.

Assumption 3.1. The function $f(\cdot, \cdot)$ described in (6–7) satisfies a Lipschitz condition with respect to its arguments over some fairly large domain $\mathbb{D}_{\mathbb{L}}$ with Lipschitz constants \bar{L}_1, \bar{L}_2 , i.e.,

$$\|f(z_1, a_1) - f(z_2, a_2)\| \leq \bar{L}_1 \|z_1 - z_2\| + \bar{L}_2 \|a_1 - a_2\| \quad (8)$$

$\forall t \in \mathbb{R}^+ \cup \{0\}$; $z_1, z_2, a_1, a_2 \in \mathbb{D}_{\mathbb{L}}$ and $\bar{L}_1, \bar{L}_2 \in \mathbb{R}^+$. Thus, we say the function $f(\cdot, \cdot)$ is locally Lipschitz.

4. Controller synthesis

The crucial aim of this study is to ensure accurate trajectory tracking of the leader agent by other agents in finite time keeping computational expenses to a minimum. Using only local communication, the consensus tracking aims to maintain follower's states in consistence with leader's states in finite time. However, the leader moves independently of followers.

4.1. Problem formulation

Let us define the position tracking error for i^{th} agent as

$$e_{x_i}(t) = x_i(t) - x_0(t), \quad (9)$$

and the velocity tracking error for i^{th} agent as

$$e_{v_i}(t) = v_i(t) - v_0(t). \quad (10)$$

In terms of graph theory, the error candidates have been modified as [28]

$$\bar{e}_{x_i}(t) = (\mathcal{L} + \mathcal{B})e_{x_i}(t) = (\mathcal{L} + \mathcal{B})(x_i(t) - x_0(t)) = \mathcal{H}(x_i(t) - x_0(t)), \quad (11)$$

where $\mathcal{L} + \mathcal{B} = \mathcal{H}$ (say)

$$\bar{e}_{v_i}(t) = (\mathcal{L} + \mathcal{B})e_{v_i}(t) = (\mathcal{L} + \mathcal{B})(v_i(t) - v_0(t)) = \mathcal{H}(v_i(t) - v_0(t)). \quad (12)$$

It is now a prime requirement of the control to make these error candidates vanish or settle in close vicinity of zero as quickly as possible to ensure accurate tracking.

4.2. Controller design

Sliding mode control is a robust control and has been very popular in the control of systems where finite time reachability is desired. Thus, the controller guaranteeing finite time consensus has been fashioned on archetype of variable structure control techniques combined with event-triggering approaches. For any sliding mode controller design [63,66] is a two step process: the design of a hypergeometric sliding manifold where state trajectories are required to be confined in finite time, and a control to force the trajectories onto this surface from any arbitrary initial location in the phase plane.

Theorem 4.1. Given plant dynamics (6,7) and errors (9–12), the control law due to traditional sliding mode controller that stabilizes the system under consideration is given by

$$\begin{aligned}u_i(t) &= -\left(K\mathcal{H}^{-1} \sinh^{-1}(m + w|\sigma_i(t)|)\text{sign}(\sigma_i(t)) + f_i(x_i(t), v_i(t))\right. \\ &\quad \left.- f(x_0(t), v_0(t)) + \lambda e_{v_i} - u_0(t) + \zeta_i - \zeta_0\right)\end{aligned}\quad (13)$$

where $\sigma_i(t)$ is the sliding manifold, which is given as

$$\sigma_i(t) = \bar{e}_{v_i}(t) + \lambda \bar{e}_{x_i}(t).$$

In (13), $-K\mathcal{H}^{-1} \sinh^{-1}(m + w|\sigma_i(t)|)\text{sign}(\sigma_i(t))$ is the forcing function, also referred to as control effort or control law. The arguments of the inverse sine hyperbolic function bear the following significance. $w > 0$ is the adjustable gain which can be tuned as per design requirements and $m > 0$ is a small positive value such that the inverse sine hyperbolic function does not attain zero argument. Generally $m \ll w$. The parameter $K > 0$ facilitates additional gain tuning.

Proof. Let us begin by formulating the sliding manifold according to the theory of sliding modes.

$$\sigma_i(t) = \bar{e}_{v_i}(t) + \lambda \bar{e}_{x_i}(t) \quad (14)$$

where λ is a scalar weighting parameter.

$$\begin{aligned} \sigma_i(t) &= \bar{e}_{v_i}(t) + \lambda \bar{e}_{x_i}(t) = \mathcal{H}(v_i(t) - v_0(t)) + \lambda \mathcal{H}(x_i(t) - x_0(t)) \\ \Rightarrow \dot{\sigma}_i(t) &= \mathcal{H}(\dot{v}_i(t) - \dot{v}_0(t)) + \lambda \mathcal{H}(\dot{x}_i(t) - \dot{x}_0(t)) \\ \Rightarrow \dot{\sigma}_i(t) &= \mathcal{H}(f_i(x_i(t), v_i(t)) + u_i(t) + \zeta_i \\ &\quad - f(x_0(t), v_0(t)) - u_0(t) - \zeta_0) + \lambda \mathcal{H}(v_i(t) - v_0(t)). \end{aligned}$$

For $\dot{\sigma}_i(t) = -K \sinh^{-1}(m + w|\sigma_i(t)|) \text{sign}(\sigma_i(t))$ as the novel reaching law, we have

$$\begin{aligned} u_i(t) &= -\left(K \mathcal{H}^{-1} \sinh^{-1}(m + w|\sigma_i(t)|) \text{sign}(\sigma_i(t)) + f_i(x_i(t), v_i(t)) \right. \\ &\quad \left. - f(x_0(t), v_0(t)) + \lambda e_{v_i} - u_0(t) + \zeta_i - \zeta_0\right). \end{aligned} \quad (15)$$

This concludes the proof. \square

In general, sliding mode controllers suffer from an undesirable effect of infinite frequency oscillations, known as chattering [63]. While electronic switching systems may exploit this phenomenon, mechanical systems [50,51] may result in wear and tear. Many times, simulation engines in numerical computer analysis and modelling, as well as sampling, switching and delay caused by hardware used to realize the system also introduce chattering and result in excitation of unmodelled high frequency dynamics. This has an adverse effect on system performance like low control accuracy and different losses in circuits and system. Techniques to smoothen the control signal by making continuous approximation of the law via sigmoid functions [45,46] also exist in literature, but then there is a trade off between performance and chattering. Other methods to eliminate chattering include the use of higher order sliding mode techniques [7,15,32,35], which has also been used in some consensus problems [12,28,31]. Using the novel reaching law proposed in this work, the undesirable effect of chattering has been eliminated and the control law is fast and smooth. Moreover, this type of reaching law is smooth, also interdependence and propinquity of the unwanted chattering phenomenon with controller gain have been obviated.

Remark 4. The novel reaching law presented in Theorem 1 possesses a nonlinear gain factor and is smooth as opposed to other reaching laws appearing in the literature of sliding mode control. The law provides faster convergence to the sliding manifold based on the parameters K and w .

The inverse hyperbolic function is odd & monotonous. $\sinh^{-1}(\cdot)$ increases as its positive argument increases and decreases with decrease in its negative argument. As its argument value decreases, the value of the function approaches 0. To ascertain that the value of the function never equals 0, the parameter m comes into picture and is used as a small offset.

The time required by the control law to reach the sliding surface can be calculated as follows:

$$\begin{aligned} \therefore \dot{\sigma}_i(t) &= -K \sinh^{-1}(m + w|\sigma_i(t)|) \text{sign}(\sigma_i(t)) \\ \therefore -K \text{sign}(\sigma_i(t)) dt &= \frac{d\sigma_i(t)}{\sinh^{-1}(m + w|\sigma_i(t)|)} \\ \Rightarrow \int_0^{t_r} dt &= \frac{1}{K} \int_0^{\sigma_i(0)} \frac{\text{sign}(\sigma_i(t))}{\sinh^{-1}(m + w|\sigma_i(t)|)} d\sigma_i(t) \end{aligned} \quad (16)$$

For $\text{sign}(\sigma_i(t)) > 0$, we have

$$\int_0^{t_r} dt = \frac{1}{K} \int_0^{\sigma_i(0)} \frac{d\sigma_i(t)}{\sinh^{-1}(m + w|\sigma_i(t)|)}. \quad (17)$$

For $\text{sign}(\sigma_i(t)) < 0$, we have

$$\begin{aligned} \int_0^{t_r} dt &= -\frac{1}{K} \int_0^{\sigma_i(0)} \frac{d\sigma_i(t)}{\sinh^{-1}(m + w|\sigma_i(t)|)} \\ &= \frac{1}{K} \int_0^{-\sigma_i(0)} \frac{d\sigma_i(t)}{\sinh^{-1}(m + w|\sigma_i(t)|)}. \end{aligned} \quad (18)$$

From (17–18), the results can be combined as

$$\int_0^{t_r} dt = \frac{1}{K} \int_0^{|\sigma_i(0)|} \frac{d\sigma_i(t)}{\sinh^{-1}(m + w|\sigma_i(t)|)} \quad (19)$$

which can be further simplified as

$$t_r = \frac{1}{K} \int_0^{|\sigma_i(0)|} \frac{d\sigma_i(t)}{\sinh^{-1}(m + w|\sigma_i(t)|)}. \quad (20)$$

$$\therefore t_r = \frac{1}{Kw} \left(\chi(\sinh^{-1}(m + w|\sigma_i(0)|)) - \chi(\sinh^{-1}(m)) \right) \quad (21)$$

where $\chi(\cdot)$ denotes the *cosh integral* function. By definition,

$$\chi[z] = \gamma + \text{Ln}[z] + \int_0^z \frac{\cosh(t) - 1}{t} dt \quad (22)$$

with $\gamma = 0.577216$ as the Euler's constant.

$$\text{Thus, } t_r \propto \frac{1}{Kw}. \quad (23)$$

Hence, higher the gain parameters, lesser the convergence time.

The sudden surge of interest in the event-driven design of circuits and systems is due to enhanced performance in applications where resources are constrained. Synchronous architectures of circuits and systems have been in dominance for a long time but they prove to be sub-optimal in terms of resource utilization. Sampling the signal and transmitting the samples over the communication channel, and at the same time occupying the computational unit when the signal does not vary significantly, are evident waste of resources. In networked control system like MAS connected over shared network consists of rapid information exchange between nodes. Their resources such as bandwidth and processor time are always constrained. The exigent need for the economic use of computational and communication resources become indispensable and event-based control is expected to yield better results in such scenario. The control gets updated only when an event (noticeable change) occurs, thereby significantly minimizing computational requirement and power consumption. The event-based control is a good candidate if the requirement is to execute different task in time-shared manner and also where control is expensive. It is also advantageous in situations when steady state needs to be upper bounded at start regardless of initial conditions and the behaviour of state evolution.

Event-based sampling has often been described as an alternative to periodic sampling. Next sample instant is dependent on the triggering of an *event*. Hence, the control law or control protocol given in (15) is modified for $\forall t \in [t^k, t^{k+1}[$ to incorporate event-based strategies.

A simplified block diagram depicting event-based strategy has been shown in Fig. 1. Solid lines represent continuous signals and dashed lines represent signals at $t = t^k$ instants. The errors introduced as a consequence of discretization of the control are

$$\bar{e}_x(t) = x(t) - x(t^k), \quad (24)$$

$$\bar{e}_v(t) = v(t) - v(t^k) \quad (25)$$

such that at t^k , $\bar{e}(t) = 0$. It should be noted that t_i^k is the triggering instant for i th agent. Note that henceforth $\bar{e}_0(t)$ and $\bar{e}_i(t)$ shall correspond to the error described by (24,25) for leader and follower agents, respectively.

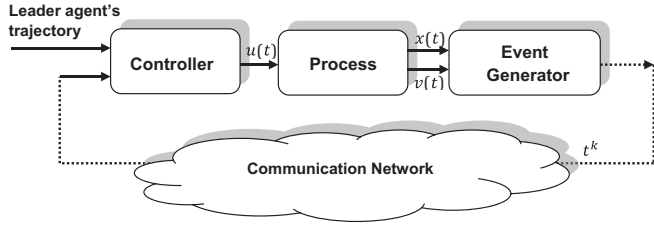


Fig. 1. Simplified block diagram of event-based strategy in leader-follower consensus tracking.

From (9–10),

$$e_{x_i}(t) = x_i(t) - x_0(t) \Rightarrow e_{x_i}(t^k) = x_i(t^k) - x_0(t^k), \quad (26)$$

$$e_{v_i}(t) = v_i(t) - v_0(t) \Rightarrow e_{v_i}(t^k) = v_i(t^k) - v_0(t^k). \quad (27)$$

Similarly, let us define

$$\tilde{e}_{x_i}(t) = e_{x_i}(t) - e_{x_i}(t^k), \quad (28)$$

$$\tilde{e}_{v_i}(t) = e_{v_i}(t) - e_{v_i}(t^k). \quad (29)$$

Theorem 4.2. Consider the system described by (6,7), error candidates (9–12), (24–29), sliding manifold (hyperplane) σ_i of (14) in the notions of sliding mode and control law of (13).

- (i) Sliding mode is said to exist in vicinity of the sliding manifold if the manifold is an essential attractor. In other words, reachability to the manifold is ascertained for some reachability constant $\eta > 0$.
- (ii) The event-triggered sliding mode control protocol (31) provides stability to the system in the sense of Lyapunov if gain K is selected as

$$K > \sup \left\{ \bar{L}_1 \|\mathcal{H}\| \|\tilde{e}_{x_i}(t)\| + \bar{L}_2 \|\mathcal{H}\| \|\tilde{e}_{v_i}(t)\| + \bar{L}_3 \|\mathcal{H}\| \|\tilde{e}_{x_0}(t)\| + \bar{L}_4 \|\mathcal{H}\| \|\tilde{e}_{v_0}(t)\| + |\lambda| \|\mathcal{H}\| \|\tilde{e}_{v_i}(t)\| \right\}. \quad (30)$$

The control protocol used to drive the states onto the sliding manifold is given as

$$u_i(t) = -\left(K\mathcal{H}^{-1} \sinh^{-1}(m + w|\sigma_i(t^k)|)\text{sign}(\sigma_i(t^k)) + f_i(x_i(t^k), v_i(t^k)) - f(x_0(t^k), v_0(t^k)) + \lambda e_{v_i}(t^k) - u_0(t) + \varsigma_i - \varsigma_0\right). \quad (31)$$

Proof. (i) Let us consider a Lyapunov candidate V such that

$$V = \frac{1}{2} \sigma_i^T(t) \sigma_i(t). \quad (32)$$

Time derivative of this candidate, given in (32) for $t \in [t^k, t^{k+1}[$ along the state trajectories yield

$$\begin{aligned} \dot{V} &= \sigma_i^T(t) \dot{\sigma}_i(t) = \sigma_i^T(t) \mathcal{H}(\dot{v}_i(t) - \dot{v}_0(t)) + \lambda \mathcal{H}(\dot{x}_i(t) - \dot{x}_0(t)) \\ &= \sigma_i^T(t) \mathcal{H}(f_i(x_i(t), v_i(t)) + u_i(t) + \varsigma_i - f(x_0(t), v_0(t)) - u_0(t) - \varsigma_i) + \lambda(v_i(t) - v_0(t)). \end{aligned} \quad (33)$$

Now, (33) can be further simplified by substituting the event-based control protocol (31). Hence,

$$\begin{aligned} \dot{V} &= \sigma_i^T(t) \mathcal{H}(f_i(x_i(t), v_i(t)) - f_i(x_i(t^k), v_i(t^k)) - K\mathcal{H}^{-1} \sinh^{-1}(m + w|\sigma_i(t^k)|)\text{sign}(\sigma_i(t^k)) \\ &\quad + f(x_0(t^k), v_0(t^k)) - \lambda e_{v_i}(t^k) + \lambda e_{v_i}(t) - f(x_0(t), v_0(t))) \\ &= \sigma_i^T(t) \mathcal{H}(-K\mathcal{H}^{-1} \sinh^{-1}(m + w|\sigma_i(t^k)|)\text{sign}(\sigma_i(t^k)) \\ &\quad + f_i(x_i(t), v_i(t)) - f_i(x_i(t^k), v_i(t^k)) \\ &\quad + f(x_0(t^k), v_0(t^k)) - f(x_0(t), v_0(t)) - \lambda e_{v_i}(t^k) + \lambda e_{v_i}(t)) \end{aligned}$$

$$\begin{aligned} &\leq \sigma_i^T(t) \mathcal{H}(-K\mathcal{H}^{-1} \sinh^{-1}(m + w|\sigma_i(t^k)|)\text{sign}(\sigma_i(t^k)) \\ &\quad + \bar{L}_1 \|x_i(t) - x_i(t^k)\| + \bar{L}_2 \|v_i(t) - v_i(t^k)\| + \bar{L}_3 \|x_0(t) - x_0(t^k)\| + \bar{L}_4 \|v_0(t) - v_0(t^k)\| \\ &\quad + |\lambda| \|e_{v_i}(t) - e_{v_i}(t^k)\|) \\ &\leq \sigma_i^T(t) \mathcal{H}(-K\mathcal{H}^{-1} \sinh^{-1}(m + w|\sigma_i(t^k)|)\text{sign}(\sigma_i(t^k)) \\ &\quad + \bar{L}_1 \|\tilde{e}_{x_i}(t)\| + \bar{L}_2 \|\tilde{e}_{v_i}(t)\| + \bar{L}_3 \|\tilde{e}_{x_0}(t)\| + \bar{L}_4 \|\tilde{e}_{v_0}(t)\| + |\lambda| \|\tilde{e}_{v_i}(t)\|) \\ &\leq \sigma_i^T(t) (-K \sinh^{-1}(m + w|\sigma_i(t^k)|)\text{sign}(\sigma_i(t^k)) \\ &\quad + \bar{L}_1 \|\mathcal{H}\| \|\tilde{e}_{x_i}(t)\| + \bar{L}_2 \|\mathcal{H}\| \|\tilde{e}_{v_i}(t)\| + \bar{L}_3 \|\mathcal{H}\| \|\tilde{e}_{x_0}(t)\| + \bar{L}_4 \|\mathcal{H}\| \|\tilde{e}_{v_0}(t)\| + |\lambda| \|\mathcal{H}\| \|\tilde{e}_{v_i}(t)\|). \end{aligned} \quad (34)$$

As long as $\sigma_i(t) > 0$ or $\sigma_i(t) < 0$, the condition $\text{sign}(\sigma_i(t)) = \text{sign}(\sigma_i(t^k))$ is strictly met $\forall t \in [t^k, t^{k+1}[$. Also $\sinh^{-1}(\cdot) > 0$ due to the nature of its arguments. Hence, when trajectories are just outside the sliding surface,

$$\begin{aligned} \dot{V} &\leq -K \sinh^{-1}(m + w|\sigma_i(t^k)|)\|\sigma_i(t)\| + \bar{L}_1 \|\sigma_i(t)\| \|\mathcal{H}\| \|\tilde{e}_{x_i}(t)\| \\ &\quad + \bar{L}_2 \|\sigma_i(t)\| \|\mathcal{H}\| \|\tilde{e}_{v_i}(t)\| + \bar{L}_3 \|\sigma_i(t)\| \|\mathcal{H}\| \|\tilde{e}_{x_0}(t)\| \\ &\quad + \bar{L}_4 \|\sigma_i(t)\| \|\mathcal{H}\| \|\tilde{e}_{v_0}(t)\| + |\lambda| \|\sigma_i(t)\| \|\mathcal{H}\| \|\tilde{e}_{v_i}(t)\| \\ &\leq \|\sigma_i(t)\| (-K \sinh^{-1}(m + w|\sigma_i(t^k)|) + \bar{L}_1 \|\mathcal{H}\| \|\tilde{e}_{x_i}(t)\| \\ &\quad + \bar{L}_2 \|\mathcal{H}\| \|\tilde{e}_{v_i}(t)\| + \bar{L}_3 \|\mathcal{H}\| \|\tilde{e}_{x_0}(t)\| + \bar{L}_4 \|\mathcal{H}\| \|\tilde{e}_{v_0}(t)\| + |\lambda| \|\mathcal{H}\| \|\tilde{e}_{v_i}(t)\|) \\ &\Rightarrow \dot{V} \leq -\eta \|\sigma_i(t)\|, \end{aligned} \quad (35)$$

where $\eta > 0$ and

$$K > \sup \left\{ \bar{L}_1 \|\mathcal{H}\| \|\tilde{e}_{x_i}(t)\| + \bar{L}_2 \|\mathcal{H}\| \|\tilde{e}_{v_i}(t)\| + \bar{L}_3 \|\mathcal{H}\| \|\tilde{e}_{x_0}(t)\| + \bar{L}_4 \|\mathcal{H}\| \|\tilde{e}_{v_0}(t)\| + |\lambda| \|\mathcal{H}\| \|\tilde{e}_{v_i}(t)\| \right\}. \quad (36)$$

This confirms that the sliding manifold is an attractor and state trajectories continuously decrease towards it $\forall t \in [t^k, t^{k+1}[$. This completes the proof of reachability. \square

Proof. (ii) Now the negative definiteness of the time derivative of (35) remains to be shown to ascertain stability in the sense of Lyapunov. At instant t^k , the control signal gets updated, thereby nullifying the discretization errors.

$$\tilde{e}_{x_i}(t) = x_i(t) - x_i(t^k) \Rightarrow \tilde{e}_{x_i}(t^k) = x_i(t^k) - x_i(t^k) = 0, \quad (37)$$

$$\tilde{e}_{v_i}(t) = v_i(t) - v_i(t^k) \Rightarrow \tilde{e}_{v_i}(t^k) = v_i(t^k) - v_i(t^k) = 0, \quad (38)$$

$$\tilde{e}_{x_0}(t) = x_0(t) - x_0(t^k) \Rightarrow \tilde{e}_{x_0}(t^k) = x_0(t^k) - x_0(t^k) = 0, \quad (39)$$

$$\tilde{e}_{v_0}(t) = v_0(t) - v_0(t^k) \Rightarrow \tilde{e}_{v_0}(t^k) = v_0(t^k) - v_0(t^k) = 0, \quad (40)$$

$$\tilde{e}_{v_i}(t) = e_{v_i}(t) - e_{v_i}(t^k) \Rightarrow \tilde{e}_{v_i}(t^k) = e_{v_i}(t^k) - e_{v_i}(t^k) = 0. \quad (41)$$

$\therefore \sinh^{-1}(\cdot) > 0$ due to the nature of its arguments, we have, from (35) and (37–41)

$$\dot{V} < 0, \quad (42)$$

assuring stability in the sense of Lyapunov. This concludes the proof of stability. \square

Remark 5. For time instants between $[t^k, t^{k+1}[$ the states show a tendency to deviate from the sliding manifold but remain bounded within a band near the manifold. The triggering instant t^k is completely characterized by a triggering rule. Next sampling instant is by virtue of this criterion. As long as this criterion is respected,

next clock pulse is not called upon and the control signal is maintained constant at the previous value. A novel triggering rule has been used in this study and is given by

$$\begin{aligned} \delta = & \alpha_1 \|e_{x_i}\|^{\beta_1} + \alpha_2 \|e_{v_i}\|^{\beta_1} \\ & - \alpha_1 \left(\left\| \sum_{j=1}^N a_{ij}(x_i(t) - x_j(t)) + b_i(x_i(t) - x_0(t)) \right\|^{\beta_1} \right) \\ & - \alpha_2 \left(\left\| \sum_{j=1}^N a_{ij}(v_i(t) - v_j(t)) + b_i(v_i(t) - v_0(t)) \right\|^{\beta_1} \right) \\ & - (c_0 + c_1 e^{-\beta_2 t}). \end{aligned} \quad (43)$$

This triggering is dynamic in nature. For each $i \in [1, N]$, j attains values $1, 2, \dots, N$. Parameters $\alpha_1, \alpha_2, \beta_1, \beta_2, c_0$ and c_1 are design parameters such that

$\alpha_1 > 0, \alpha_2 > 0, \beta_1 > 0, \beta_2 > 0, c_0 > 0, c_1 \geq 0$. a_{ij} are corresponding entries of adjacency matrix \mathcal{A} .

Remark 6. In this study, each follower agent is triggered asynchronously based on local information only, and the leader agent is not triggered. Thus, $u_0(t) = u_0(t^k)$, $x_0(t) = x_0(t^k)$ and $v_0(t) = v_0(t^k)$.

Theorem 4.3. Consider the system described by (7), the control protocol (31) and the discretization errors (24–29). The sequence of triggering instants $\{t_i^k\}_{k=0}^\infty$ for each follower agent respects the triggering rule given in (43). The inter event execution time T_i^k time in case of this aperiodic triggering is bounded below by a finite positive quantity ϕ . Consequently, Zeno phenomenon, i.e., accumulation of events at the same instant (inter event time is infinitely small that sampling is done infinitely fast) is excluded.

Proof. The control protocol (31) is recalled here as

$$\begin{aligned} u_i(t) = & -(K\mathcal{H}^{-1} \sinh^{-1}(m + w|\sigma_i(t^k)|)\text{sign}(\sigma_i(t^k)) \\ & + f_i(x_i(t^k), v_i(t^k)) - f(x_0(t^k), v_0(t^k)) + \lambda e_{v_i}(t^k) \\ & - u_0(t) + \varsigma_i - \varsigma_0), \end{aligned} \quad (44)$$

which can also be expressed as

$$\begin{aligned} u_i(t) = & -(K\mathcal{H}^{-1} \sinh^{-1}(m + w|\sigma_i(t^k)|)\text{sign}(\sigma_i(t^k)) + \tilde{\lambda} f_i(X_i(t^k)) \\ & - f(x_0(t), v_0(t)) + \lambda \mathcal{H} v_0(t) - u_0(t) - \varsigma_0), \end{aligned} \quad (45)$$

where $\tilde{\lambda} = [\lambda \quad 1]$ and $f_i(X_i) = \begin{bmatrix} f_i(x_i, v_i) \\ \varsigma_i \end{bmatrix}$.

The system (7) can also be expressed without loss of generality as

$$\dot{X}_i = f_i(X_i(t)) + \tilde{B}_i u_i(t), \quad (46)$$

with $X_i = [x_i \quad v_i]^T$, $f_i(X_i)$ as in $\begin{bmatrix} f_i(x_i, v_i) \\ \varsigma_i \end{bmatrix}$ and $\tilde{B}_i = [0 \quad 1]^T$.

Let us define

$$\hat{e}_i(t) = [\bar{e}_{x_i}(t) \quad \bar{e}_{v_i}(t)]^T. \quad (47)$$

Next we define the inter event execution time $T_i^k = t_i^{k+1} - t_i^k$ as the time it takes for $\|\hat{e}_i\|$ to rise from 0 to $\|\hat{e}_i\|_\infty$ for $(k+1)^{th}$ execution of the control signal (31). Thus, between k^{th} and $(k+1)^{th}$ sampling instant in the execution of control, the discretization error is non zero. We can write $\forall t \in [t_i^k, t_i^{k+1}]$

$$\frac{d}{dt} \|\hat{e}_i(t)\| \leq \left\| \frac{d}{dt} \hat{e}_i(t) \right\| \leq \left\| \frac{d}{dt} X_i(t) \right\|$$

$$\Rightarrow \left\| \frac{d}{dt} \hat{e}_i(t) \right\| \leq \|f_i(X_i(t)) + \tilde{B}_i u_i(t)\|$$

Substituting the control protocol expressed in (45) in the above inequality, we get

$$\begin{aligned} \left\| \frac{d}{dt} \hat{e}_i(t) \right\| \leq & \|f_i(X_i(t)) - K\tilde{B}_i \mathcal{H}^{-1} \sinh^{-1}(m + w|\sigma_i(t^k)|)\text{sign}(\sigma_i(t^k)) \\ & - \tilde{\lambda} \tilde{B}_i f_i(X_i(t^k)) - \tilde{B}_i f(x_0(t), v_0(t)) \\ & + \lambda \tilde{B}_i \mathcal{H} v_0(t) - \tilde{B}_i u_0(t) - \tilde{B}_i \varsigma_0\| \end{aligned} \quad (48)$$

$$\begin{aligned} \leq & \|f(X_i(t))\| + \|K\tilde{B}_i \mathcal{H}^{-1} \sinh^{-1}(m + w|\sigma_i(t^k)|)\text{sign}(\sigma_i(t^k))\| \\ & + \|\tilde{\lambda} \tilde{B}_i f_i(X_i(t^k))\| + \|\tilde{B}_i f(x_0(t), v_0(t))\| \\ & + \|\lambda \tilde{B}_i \mathcal{H} v_0(t)\| + \|\tilde{B}_i u_0(t)\| + \|\tilde{B}_i \varsigma_0\| \\ \leq & \|f_i(X_i(t))\| + \|K\tilde{B}_i \mathcal{H}^{-1} \sinh^{-1}(m + w|\sigma_i(t^k)|)\text{sign}(\sigma_i(t^k))\| \\ & + \|\tilde{\lambda} \tilde{B}_i f_i(X_i(t^k))\| + F \end{aligned} \quad (49)$$

where $F = \|\tilde{B}_i f(x_0(t), v_0(t))\| + \|\lambda \tilde{B}_i \mathcal{H} v_0(t)\| + \|\tilde{B}_i u_0(t)\| + \|\tilde{B}_i \varsigma_0\|$. Further simplification of (49) results in

$$\begin{aligned} \left\| \frac{d}{dt} \hat{e}_i(t) \right\| \leq & \bar{L} \|X_i(t)\| + \|\tilde{\lambda} \tilde{B}_i f_i(X_i(t^k))\| + F \\ & + |K| \|\tilde{B}_i \mathcal{H}^{-1} \sinh^{-1}(m + w|\sigma_i(t^k)|)\| \end{aligned} \quad (50)$$

$$\begin{aligned} \leq & \bar{L} \|X_i(t^k) + \hat{e}_i(t)\| + \|\tilde{\lambda} \tilde{B}_i\| \bar{L} \|X_i(t^k)\| + F \\ & + |K| \|\tilde{B}_i \mathcal{H}^{-1} \sinh^{-1}(m + w|\sigma_i(t^k)|)\| \\ \leq & \bar{L} \|\hat{e}_i(t)\| + \bar{L}(1 + \|\tilde{\lambda} \tilde{B}_i\|) \|X_i(t^k)\| + \Omega \leq \bar{L} \|\hat{e}_i(t)\| + \bar{\upsilon} + \Omega \end{aligned} \quad (51)$$

where $\Omega = |K| \|\tilde{B}_i \mathcal{H}^{-1} \sinh^{-1}(m + w|\sigma_i(t^k)|)\| + F$ and $\bar{\upsilon} = \bar{L}(1 + \|\tilde{\lambda} \tilde{B}_i\|) \|X_i(t^k)\|$ are positive quantities.

For $t \in [t_i^k, t_i^{k+1}]$, the solution to the differential inequality (51) can be understood by using Comparison Lemma [22] with initial condition $\|\hat{e}_i(t)\| = 0$. Comparison Lemma [22,36] is found to be particularly useful when information on bounds on the solution is more crucial than the solution itself.

$\because \Omega$ and $\bar{\upsilon}$ are always positive, the solution to the differential inequality of (51) comes out to be a finite positive value [18]. Thus,

$$\|\hat{e}_i(t)\| \leq \phi; \quad \phi \in \mathbb{R}^+. \quad (52)$$

This implies that T_i^k is always bounded below by some finite positive quantity, and hence the proof is concluded. \square

Remark 7. The results established in Theorem 4 hold locally over some fairly large compact domain \mathbb{D}_L . Under varied settings, the desired closed-loop performance can be achieved by tuning the design parameters properly. From (44), as long as $\delta < 0$, next sample is not taken and we say that the system is delivering acceptable closed-loop performance.

Remark 8. During sampling, a finite but not necessarily constant delay Δ is unavoidable due to hardware characteristics. In such cases the control is held constant $\forall t_i \in [t_i^k + \Delta, t_i^{k+1} + \Delta]$. In this work, we have assumed that Δ is negligible and hence, is neglected harmlessly. Hence for our case, control is constant in the interval $[t_i^k, t_i^{k+1}]$.

Definition 4.4. The triggering rule that governs the closed-loop performance of the system has been presented in (43) as

$$\delta = \alpha_1 \|e_{x_i}\|^{\beta_1} + \alpha_2 \|e_{v_i}\|^{\beta_1}$$

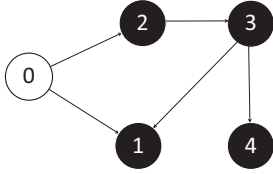


Fig. 2. Digraph topology of the MAS- leader represented with 0 and followers represented with 1, 2, 3 and 4.

$$\begin{aligned}
 & -\alpha_1 \left(\left\| \sum_{j=1}^N a_{ij}(x_i(t) - x_j(t)) + b_i(x_i(t) - x_0(t)) \right\|^{\beta_1} \right) \\
 & -\alpha_2 \left(\left\| \sum_{j=1}^N a_{ij}(v_i(t) - v_j(t)) + b_i(v_i(t) - v_0(t)) \right\|^{\beta_1} \right) \\
 & -(c_0 + c_1 e^{-\beta_2 t}).
 \end{aligned} \quad (53)$$

We can now define the proposed triggering rule presented in (43) and recalled in (53) in an iterative fashion. As long as $\delta < 0$, the desired closed-loop performance is said to be maintained. When $\delta > 0$, the control protocol is activated. Hence, iteratively

$$t_i^{k+1} = \inf\{t_i \in [t_i^k, \infty[: \delta \geq 0\} \quad (54)$$

determines the instants at which new samples are taken.

5. Results and discussions

The communication topology that is used for information exchange among agents is shown in Fig. 2 and is directed in nature. The matrices associated with the topology under consideration are given below.

$$\begin{aligned}
 \mathcal{A} &= \begin{bmatrix} 0 & 0 & 1 & 0 \\ 0 & 0 & 0 & 0 \\ 0 & 1 & 0 & 0 \\ 0 & 0 & 1 & 0 \end{bmatrix} & \mathcal{B} &= \begin{bmatrix} 1 & 0 & 0 & 0 \\ 0 & 1 & 0 & 0 \\ 0 & 0 & 0 & 0 \\ 0 & 0 & 0 & 0 \end{bmatrix} \\
 \mathcal{D} &= \begin{bmatrix} 1 & 0 & 0 & 0 \\ 0 & 0 & 0 & 0 \\ 0 & 0 & 1 & 0 \\ 0 & 0 & 0 & 1 \end{bmatrix} & & (55)
 \end{aligned}$$

$$\begin{aligned}
 \mathcal{L} = \mathcal{D} - \mathcal{A} &= \begin{bmatrix} 1 & 0 & -1 & 0 \\ 0 & 0 & 0 & 0 \\ 0 & -1 & 1 & 0 \\ 0 & 0 & -1 & 1 \end{bmatrix} \\
 \mathcal{L} + \mathcal{B} &= \begin{bmatrix} 2 & 0 & -1 & 0 \\ 0 & 1 & 0 & 0 \\ 0 & -1 & 1 & 0 \\ 0 & 0 & -1 & 1 \end{bmatrix}
 \end{aligned} \quad (56)$$

The topology shown for demonstration bears Laplacian with real eigenvalues. It is worthy to note that the same discussion applies and can be extended to Laplacian with complex eigenvalues too.

Dynamics of the leader and follower agents considered here are described as

$$\dot{x}_0 = v_0, \quad (57)$$

$$\dot{v}_0 = u_0 \cos(t) + 0.2 \sin(x_0) + \varsigma_0, \quad (58)$$

where u_0 is the control input of the leader and is taken to be

$$u_0 = \frac{2 \cos(0.1\pi t)}{1 + e^{-t}}. \quad (59)$$

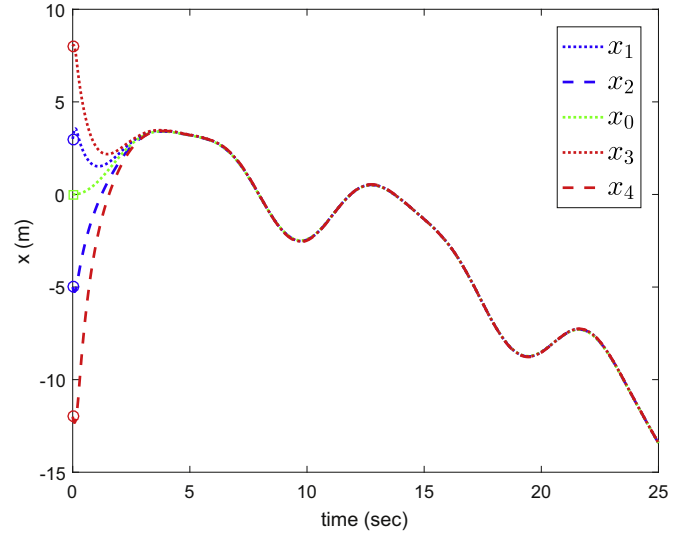


Fig. 3. Consensus in positions along first axis.

Note that upper bounds on u_0 is finite and can be easily calculated.

$$\dot{x}_1 = v_1, \quad (60)$$

$$\dot{v}_1 = 0.1 \sin(v_1)^{1/3} + \cos^2(2\pi t) + e^{-t} + u_1(t) + \varsigma_1, \quad (61)$$

$$\dot{x}_2 = v_2, \quad (62)$$

$$\dot{v}_2 = 0.1 \sin(v_2) + \cos(2\pi t) + u_2(t) + \varsigma_2, \quad (63)$$

$$\dot{x}_3 = v_3, \quad (64)$$

$$\dot{v}_3 = -v_3 \cos(t) - \sin(x_3) - \cos(x_3) + u_3(t) + \varsigma_3, \quad (65)$$

$$\dot{x}_4 = v_4, \quad (66)$$

$$\dot{v}_4 = \sin(x_4) + \cos(e^{-v_4 t}) + u_4(t) + \varsigma_4. \quad (67)$$

These dynamics are locally Lipschitz over some fairly large domain \mathbb{D}_L . The plots of the results using the proposed control scheme have been presented in this section. Results presented in this study are of MAS in \mathbb{R}^2 . The initial conditions are taken to be large values, i.e., far away from the equilibrium point. Clearly, consensus tracking has been achieved in finite time. It should be noted that there is always some constraint on how much control authority is invoked to drive the system in consensus. This constraint usually comes from the physical nature of the actuators used in realizing the controller. In our work, we have simulated the scenario considering actuator constraints such that the maximum fluctuation of the control signal is fixed and the maximum control authority is limited by some finite value u_{max} . Mathematically, constrained control of each agent (u_{c_i}) is selected as $u_{c_i} = \min(u_{max}, |u_i|)$ such that maximum allowed fluctuation in the signal, i.e., $|u_{c_{max}} - u_{c_{min}}| = \varpi$ and $\|u_i\| \leq u_{max} \leq \varpi$. Moreover, reachability and stability in case of constrained control (u_{c_i}) can be simply ascertained from the conditions (35), (36), similar to the case of unrestricted control effort.

It is evident that the proposed control authority drives the states to consensus quickly. Figs. 3 and 4 show the consensus of position states of the follower agents to those of the leader agent along the two axes. Similarly Figs. 5 and 6 show the consensus of velocity states of the follower agents to those of the leader agent

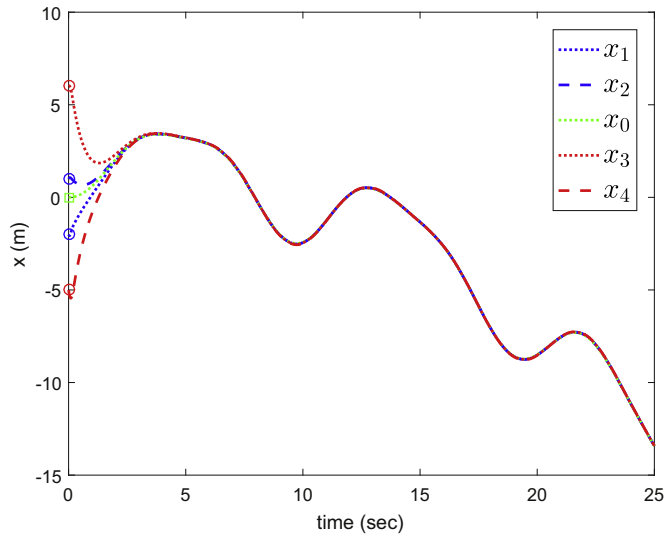


Fig. 4. Consensus in positions along second axis.

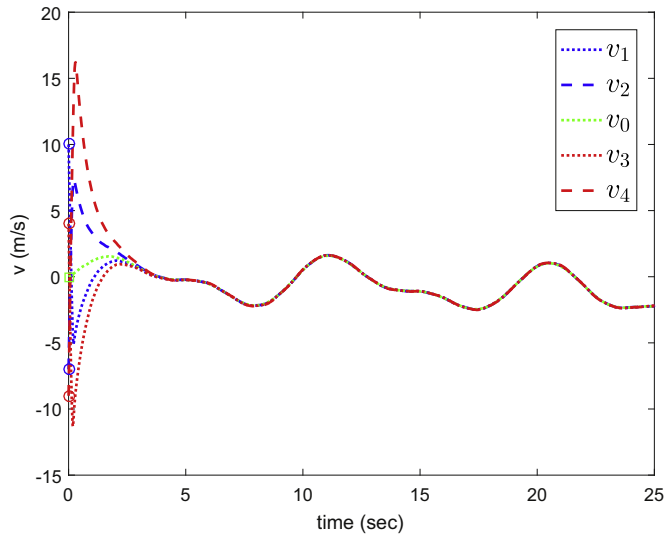


Fig. 5. Consensus in velocities along first axis.

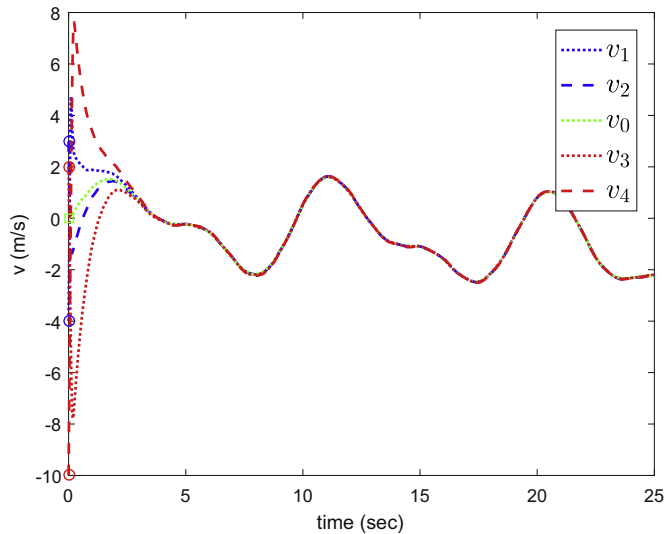


Fig. 6. Consensus in velocities along second axis.

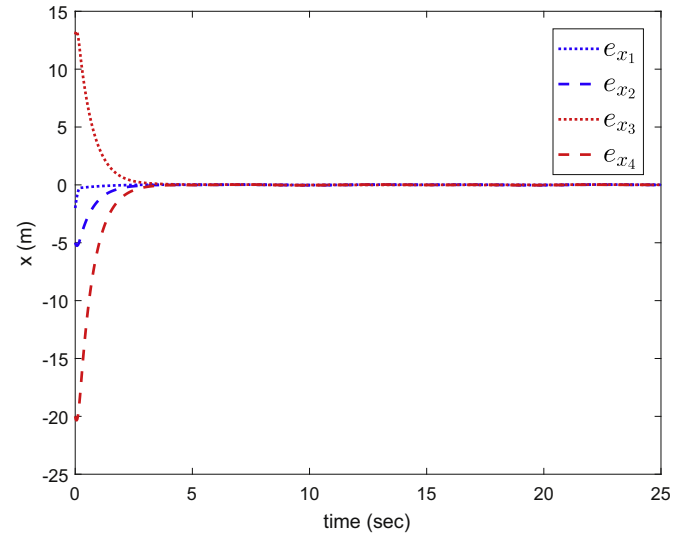


Fig. 7. Tracking errors in positions along first axis during consensus.

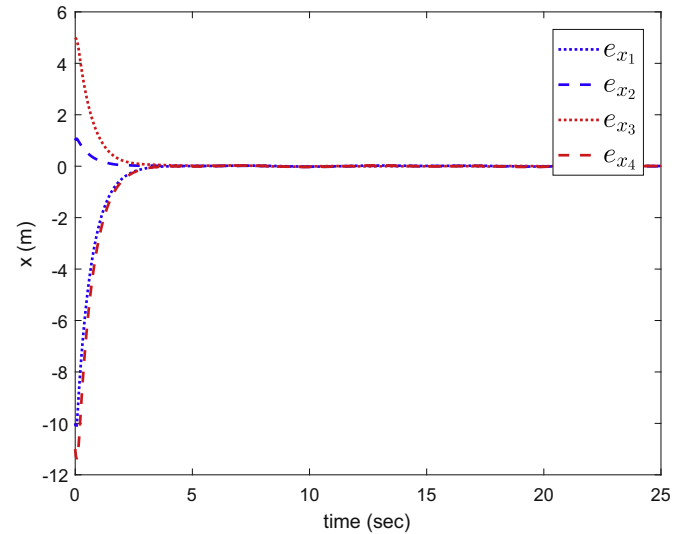


Fig. 8. Tracking errors in positions along second axis during consensus.

along the two axes. It can be inferred from Figs. 3–6 that the consensus of position and velocity of all the follower agents can be achieved with any arbitrary initial position and velocity of leader and follower agents. By adjusting the parameters w & K , the speed of convergence of follower agents to the leader's trajectory can be tailored. Faster convergence of error variables to zero as evident from Figs. 7–10 shows desirable closed-loop dynamics of the system and proves the effectiveness of the controller. It is also worthy to investigate the behavior of MAS under bounded and matched perturbations. We designate the term matched perturbations to exogenous disturbances entering the system through input channel. Sliding mode is known for its inherent robustness and is known to reject any disturbance that is matched. The effect of disturbance has been depicted in Figs. 11 and 12. In spite of slight chattering in trajectories, consensus to the leader is achieved in finite time. Figs. 13 and 14 are the plots of the sliding hyperplanes, or sliding manifolds (surface variables) for each follower agent where the trajectories are to be confined for all future time. Figs. 15 and 16 depict the control signals without actuator constraints (unrestricted control effort), which are chattering free and smooth. In practice, there are always actuation constraints, hence we have re-

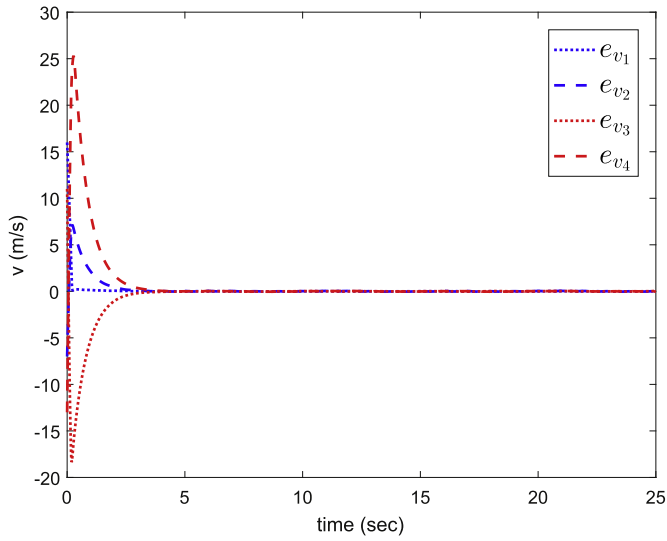


Fig. 9. Tracking errors in velocities along first axis during consensus.

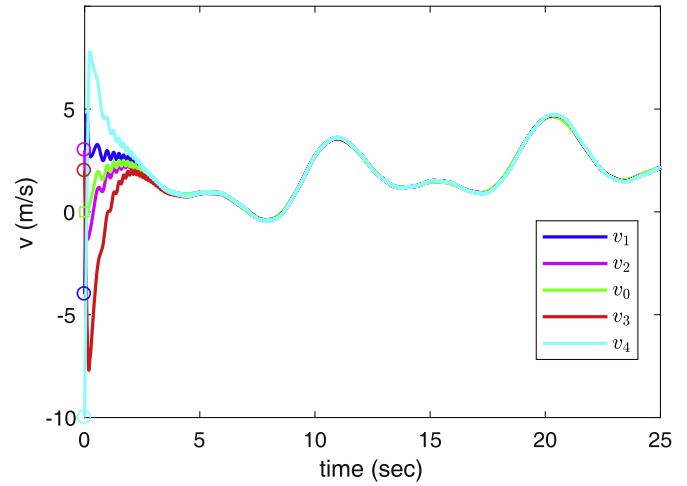


Fig. 12. Velocity consensus in mismatched disturbance along second axis.

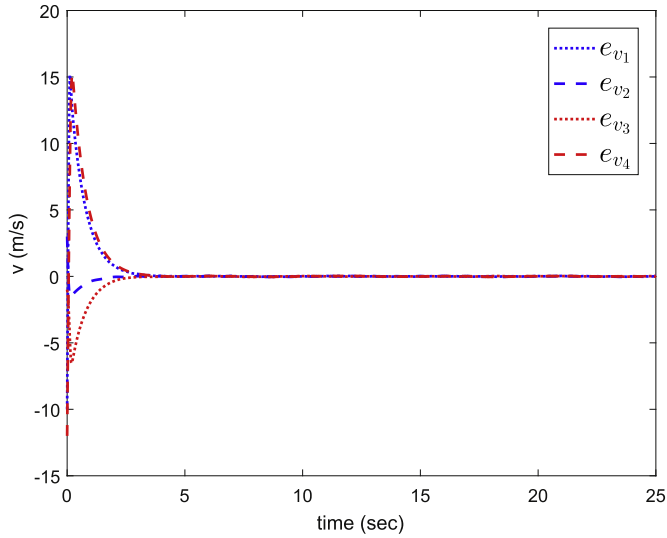


Fig. 10. Tracking errors in velocities along second axis during consensus.

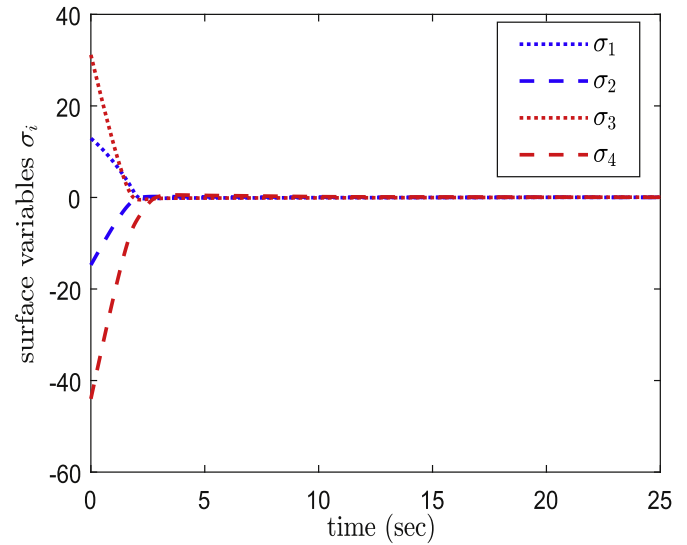


Fig. 13. Sliding manifolds along first axis during consensus.

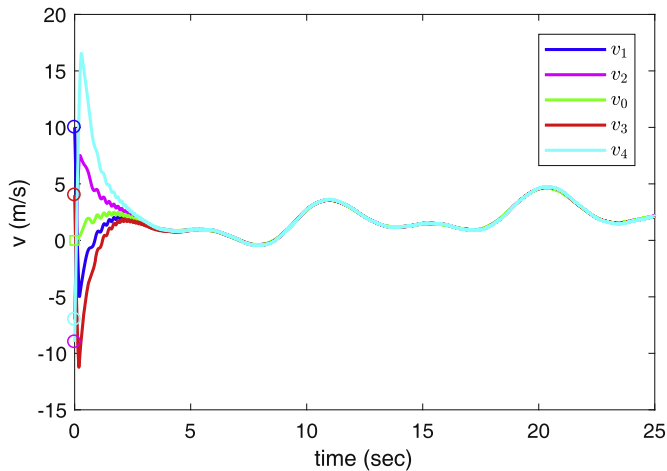


Fig. 11. Velocity consensus in mismatched disturbance along first axis.

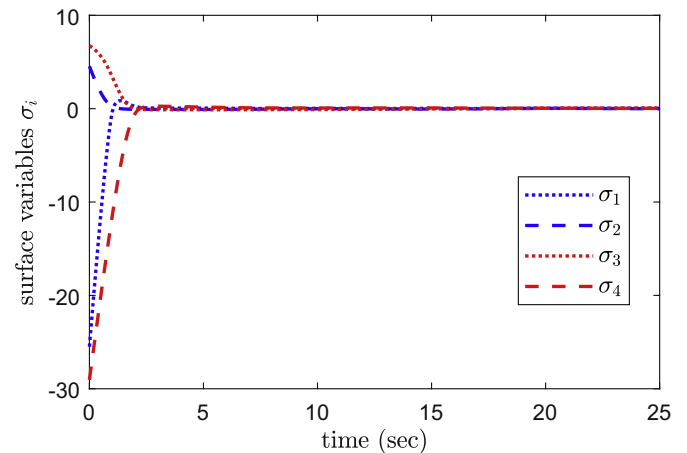


Fig. 14. Sliding manifolds along second axis during consensus.

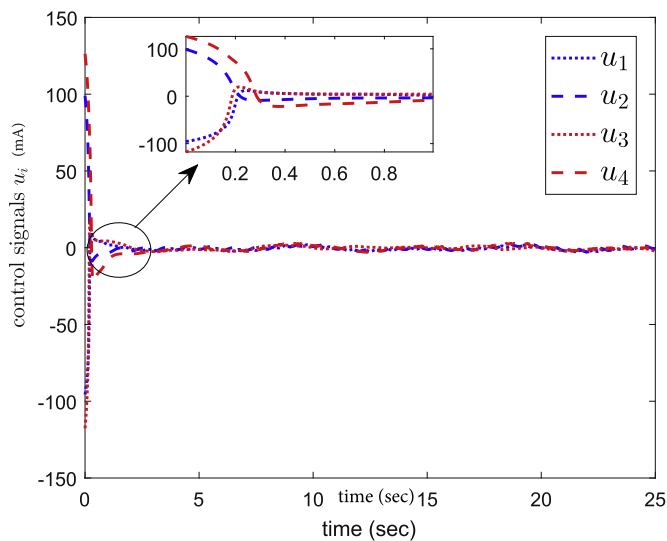


Fig. 15. Control signals along first axis during consensus.

Table 1

Parameter values used in simulation.

c_0	c_1	α_1	α_2	β_1	β_2	K	λ	m	w
10^{-4}	0.25	0.1	0.3	2	$\frac{2}{3}$	25	1.55	10^{-3}	1.774

stricted the maximum allowable fluctuation in control signal magnitude (ω) to 30 mA to test the efficacy of the proposed scheme. Restricting the amplitude of control effort only reduces the speed of consensus, while stability is not affected. It is evident from Fig. 17 that the control signals of all the followers are smooth and asymptotic stability can be guaranteed under actuation constraints also. The parametric values used in simulation are tabulated in Table (1).

Figs. 18 and 19 depict the evolution of state trajectories of both the states (position and velocity) for all the agents in the MAS during consensus. In many practical applications, it is unreasonable to permanently fix the threshold (which happens to be $c_0 + c_1 e^{-\beta_2 t}$ in this study, refer (53) and the triggering rule). Suppose there are multiple agents tasked to maintain a prescribed geometrical formation. The inter-agent communication should be maintained even after the geometrical formation is achieved, but if the threshold remains fixed at some constant value, some of the data packets containing important information on maintaining the formation may

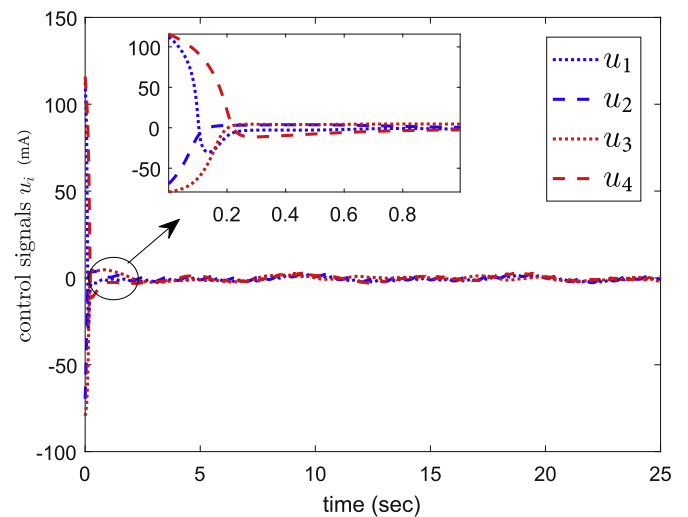


Fig. 16. Control signals along second axis during consensus.

not be triggered. Another instance is of some widely used practical communication networks such as IEEE 802.11 WLAN. This network has a time varying data transmission rate owing to variable interference and random wireless fading. It is, thus, required that the accuracy adjustment parameter (threshold) should be altered in a dynamic fashion to schedule agents' communication while ensuring resource efficiency and desired closed-loop performance. Figs. (21–24) illustrate aperiodic sampling intervals for the follower agents under the proposed triggering rule. It can be inferred from these plots that the sampling and controller update requirement has been drastically reduced in comparison to the periodic sampling and update of controllers to save energy and computational requirements without compromising the closed-loop performance of the system. Combined sampling intervals and combined sampling instants of agents are shown in Figs. 20 and 29, respectively. Maintaining formation in certain scenarios is one of the most important practical applications of MAS operation. An application of formation keeping by the follower agents along both the axes has been presented in Figs. 25 and 26 where agents maintain a predefined fixed distance among themselves. Fig. 27 presents the plot of phase plane trajectories of leader and follower agents in MAS during consensus. Fig. 28 shows the evolution of state trajectories of agents in MAS during formation.

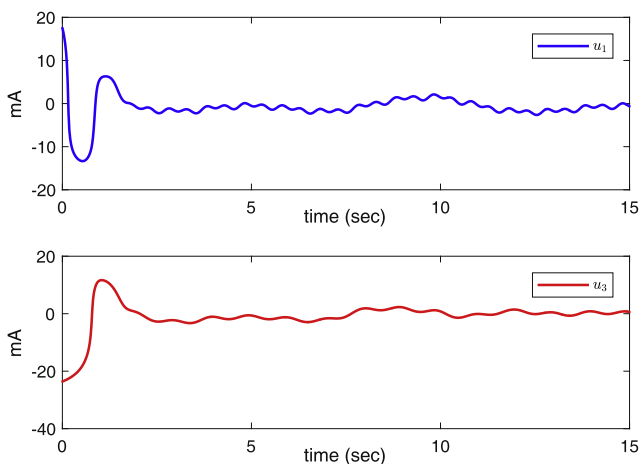
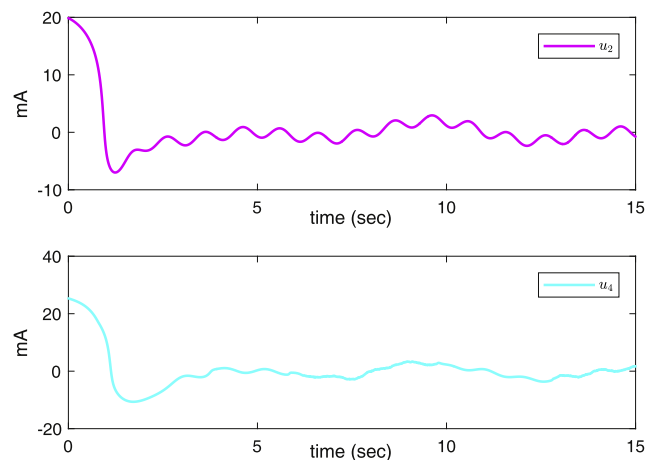


Fig. 17. Control signals under actuation constraints.



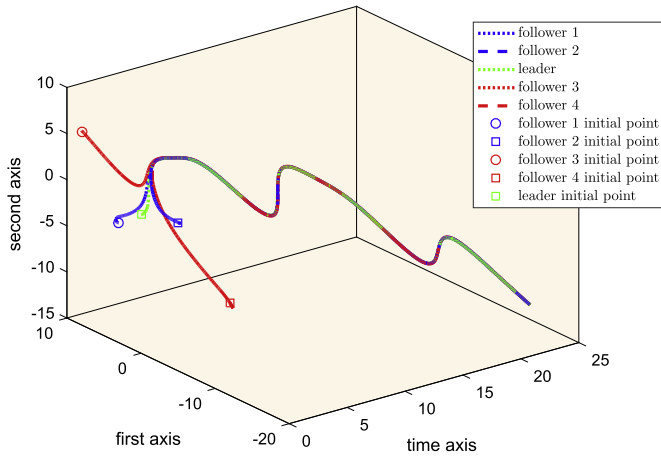


Fig. 18. Evolution of state trajectories of first state during consensus.

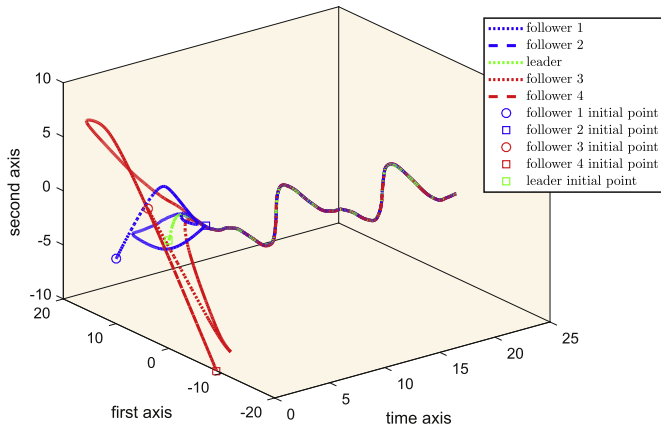


Fig. 19. Evolution of state trajectories of second state during consensus.

Initial conditions taken for simulation are $x_1(0) = [3 \ -2]^T$, $v_1(0) = [10 \ -4]^T$, $x_2(0) = [-5 \ 1]^T$, $v_2(0) = [-7 \ 3]^T$, $x_3(0) = [8 \ 6]^T$, $v_3(0) = [4 \ 2]^T$, $x_4(0) = [-12 \ -5]^T$, $v_4(0) = [-9 \ -10]^T$, $x_0(0) = [0 \ 0]^T$ and $v_0(0) = [0 \ 0]^T$. Disturbance has been accounted for as $\zeta_0 = \zeta_i = 0.3 \sin(\pi^2 t^2)$ such that $\|\zeta_{max}\|_\infty < 0.3$. This disturbance is bounded and matched.

We have used the number of controller updates as our performance metric. For sampling frequency of 1 KHz, the number of controller updates has been tabulated in Table 2. We have consid-

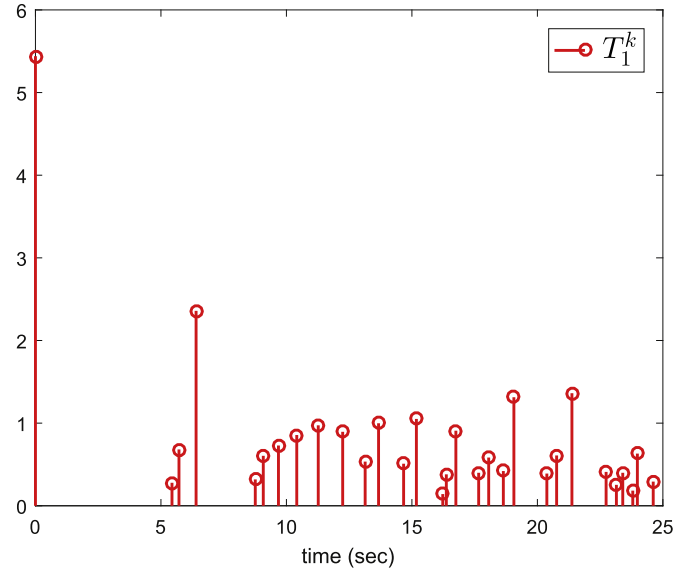


Fig. 21. Sampling interval for first follower agent.

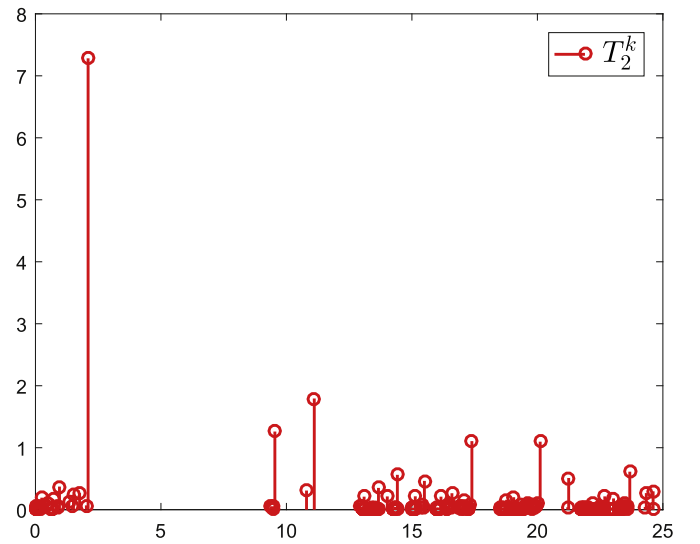


Fig. 22. Sampling interval for second follower agent.

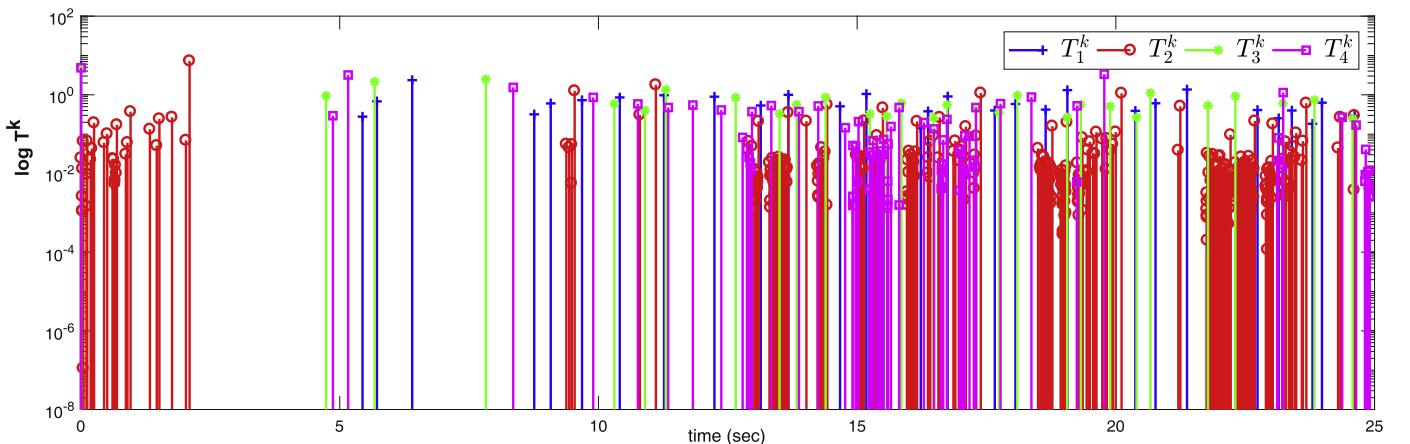


Fig. 20. Combined plot of sampling intervals.

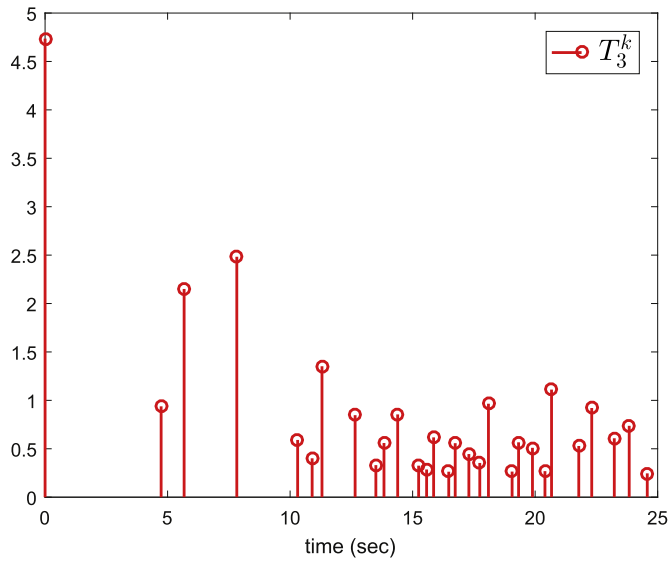


Fig. 23. Sampling interval for third follower agent.

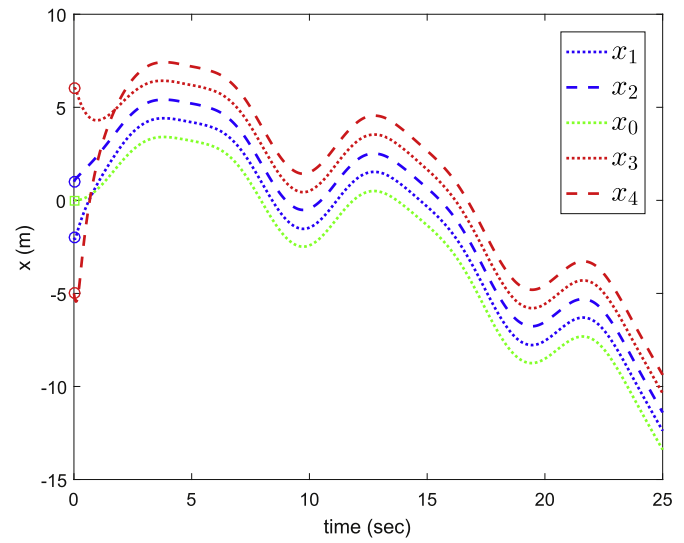


Fig. 26. Agents in formation along second axis.

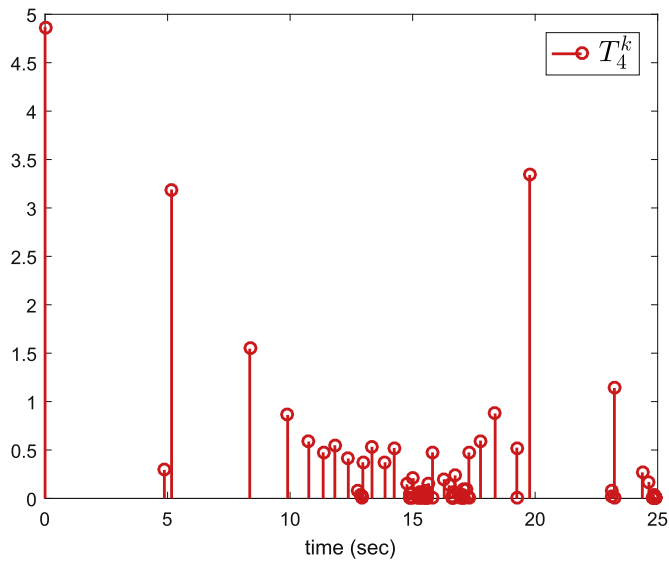


Fig. 24. Sampling interval for fourth follower agent.

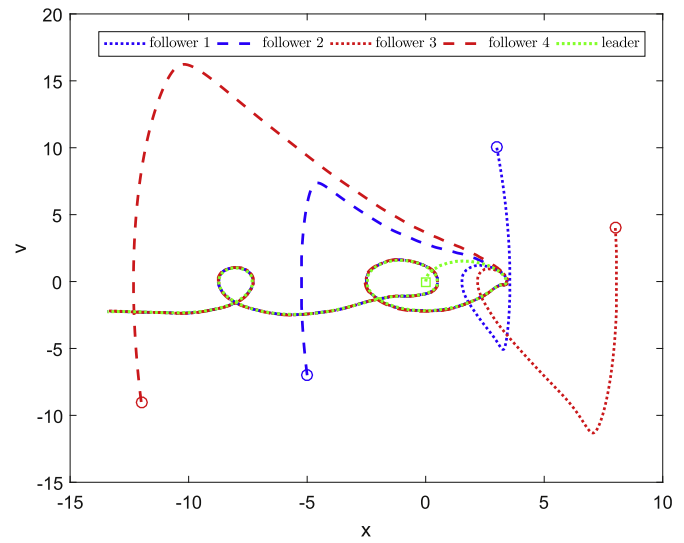


Fig. 27. Phase plane trajectory of agents during consensus.

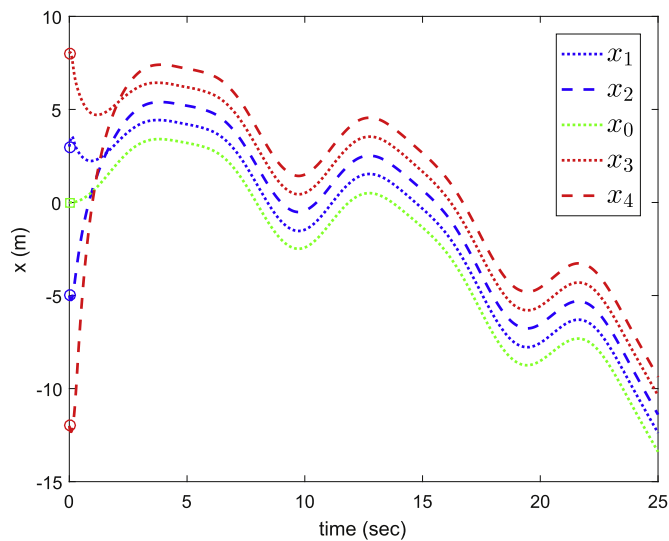


Fig. 25. Agents in formation along first axis.

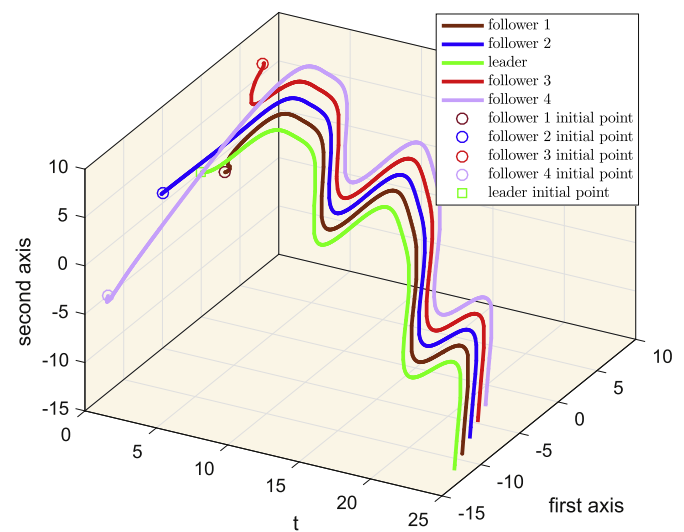


Fig. 28. Agents in formation.

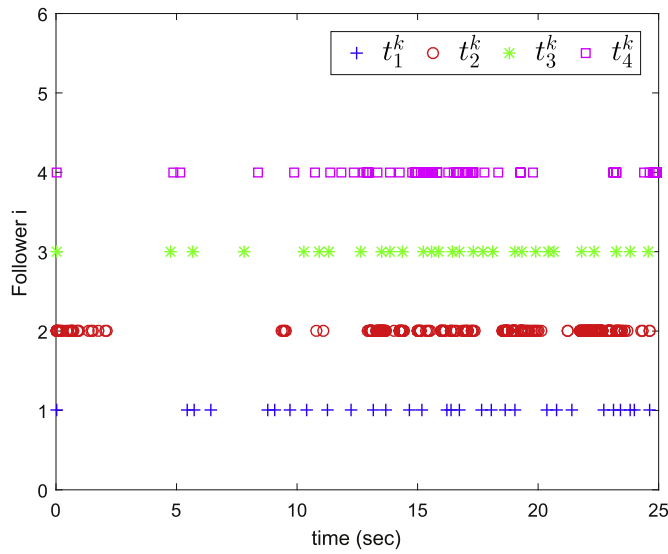


Fig. 29. Combined plot of sampling instants.

Table 2
Number of controller updates.

Agent	Follower 1	Follower 2	Follower 3	Follower 4
No. of updates	30	385	29	86
Total number of updates	530			

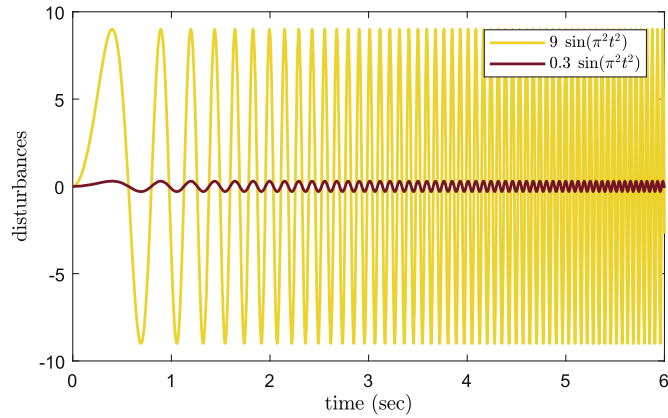


Fig. 30. Time varying disturbance.

ered energy efficiency and computational complexity in terms of number of samples taken and controller update requirements. The fewer number of sampling and control updates will consume less energy. For simulation run of 25 s, total number of controller updates are 25000 (1 KHz sampling frequency) in time-triggered scenario. However, in event-based sliding mode controller, the number of updates reduce to 530. Therefore, energy efficiency can be calculated as the ratio of updates in event-based control to the number of updates in time triggered control. In our case, the ratio is $\frac{530}{25000} = 2.12\%$. Hence, for 100 controller updates in time triggered case, only 2 updates are required in event-based case, thereby minimizing the energy expenses drastically.

Last, but not the least, Fig. 30 shows the time varying disturbance that affects the system, whose magnitude is restricted to 0.3 units for matched case and 9 units for mismatched case.

6. Concluding remarks

In this work, a novel event-triggered sliding mode controller has been synthesized to make optimal use of communication resources when heterogeneous MAS described by inherent nonlinear second order dynamics have been driven towards consensus. A finite time distributed consensus protocol for leader following MAS under directed graph topology has been proposed. The controller has been synthesized on the archetype of sliding mode control, popularly known for its inherent robustness and disturbance rejection qualities. Discontinuities in the control excite unmodelled high frequency dynamics in the system that may cause wear and tear of the actuator and other physical parts of the system and even high heat losses in electrical power circuits. Hence, an odd and monotonous function like inverse sine hyperbolic has been used to realize the sliding mode reaching law, making the gain nonlinear and removing the propinquity and interdependence of gain and chattering. Combining event-triggering scheme aided towards saving energy expenditure and reducing computational requirements. The control updates only when some noticeable measurement error crosses a designer fixed threshold while ensuring that the closed loop performance is not compromised. Negative definiteness of the Lyapunov candidate has been shown, thus ensuring stability in the sense of Lyapunov. The inter event execution time between two consecutive controller updates is lower bounded by a positive finite value to exclude Zeno behavior. Finally, simulation results of leader-following consensus and formation keeping of MAS have been presented to validate the efficiency of the proposed controller.

7. Recommendations and outlook

This study can be extended by incorporating a general design mechanism for selecting a particular triggering rule in the cases discussed in this work. Moreover, the effects of time-varying delay and missing communication can be addressed as extension to the current work.

References

- [1] A. Sinha, R.K. Mishra, Consensus in first order nonlinear heterogeneous multi-agent systems with event-based sliding mode control, *International Journal of Control* (2018), doi:10.1080/00207179.2018.1531147.
- [2] A. Anta, P. Tabuada, To sample or not to sample: Self-triggered control for nonlinear systems, *IEEE Trans. Autom. Control* 55 (9) (2010) 2030–2042.
- [3] D. Antunes, B.A. Khashooei, Consistent dynamic event-triggered policies for linear quadratic control, *IEEE Trans. Control Netw. Syst.* PP (99) (2017) 1, doi:10.1109/TCNS.2017.2713248.
- [4] A. Astolfi, L. Marconi, *Analysis and Design of Nonlinear Control Systems (In Honour of Alberto Isidori)*, Springer-Verlag, 2007.
- [5] K.J. Åström, *Event Based Control*, Springer Berlin Heidelberg, Berlin, Heidelberg, pp. 127–147.
- [6] K.J. Åström, B.M. Bernhardsson, Comparison of Riemann and Lebesgue sampling for first order stochastic systems, in: *Proceedings of the 41st IEEE Conference on Decision and Control*, 2002., 2, 2002, pp. 2011–2016vol.2, doi:10.1109/CDC.2002.1184824.
- [7] G. Bartolini, L. Fridman, A. Pisano, E. Usai (Eds.), *Modern Sliding Mode Control Theory*, Springer-Verlag, Berlin Heidelberg, 2008, doi:10.1007/978-3-540-79016-7.
- [8] A.K. Behera, B. Bandyopadhyay, Event based robust stabilization of linear systems, in: *Proceedings of the 40th Annual Conference of the IEEE Industrial Electronics Society, IECON 2014*, 2014, pp. 133–138.
- [9] B. Bollobas, *Modern Graph Theory*, Springer-Verlag, 1998. <http://www.springer.com/in/book/9780387984889>.
- [10] G. Chartrand, L. Lesniak, P. Zhang, *Graphs & Digraphs, Sixth Edition, Textbooks in Mathematics*, CRC Press- Taylor and Francis Group, 2015.
- [11] F.R.K. Chung, *Spectral Graph Theory*, CBMS Regional Conference Series in Mathematics, 92, AMS and CBMS, 1997. <http://bookstore.ams.org/cbms-92>.
- [12] J. Dávila, Distributed tracking of first order systems using second-order sliding modes, *IFAC Proc. Vol.* 47 (3) (2014) 1392–1397, doi:10.3182/20140824-6-ZA-1003.00816.
- [13] N. Deo, *Graph Theory with Applications to Engineering and Computer Science (Prentice Hall Series in Automatic Computation)*, Prentice-Hall, Inc., Upper Saddle River, NJ, USA, 1974.

- [14] Y. Dong, J. Huang, A leader-following rendezvous problem of double integrator multi-agent systems, *Automatica* 49 (5) (2013) 1386–1391, doi:[10.1016/j.automatica.2013.02.024](https://doi.org/10.1016/j.automatica.2013.02.024).
- [15] S.V. Emel'yanov, S.K. Korovin, A. Levant, High-order sliding modes in control systems, *Comput. Math. Model.* 7 (3) (1996) 294–318, doi:[10.1007/BF01128162](https://doi.org/10.1007/BF01128162).
- [16] E. Garcia, Y. Cao, D.W. Casbeer, An event-triggered control approach for the leader-tracking problem with heterogeneous agents, *Int. J. Control* 1–13, doi:[10.1080/00207179.2017.1312668](https://doi.org/10.1080/00207179.2017.1312668).
- [17] X. Ge, Q.L. Han, Distributed formation control of networked multi-agent systems using a dynamic event-triggered communication mechanism, *IEEE Trans. Ind. Electron.* PP (99) (2017) 1, doi:[10.1109/TIE.2017.2701778](https://doi.org/10.1109/TIE.2017.2701778).
- [18] A. Girard, Dynamic event generators for event-triggered control systems, *CoRR* abs/1301.2182 (2013). <http://arxiv.org/abs/1301.2182>.
- [19] J.L. Gross, J. Yellen, P. Zhang, *Handbook of Graph Theory, Second Edition, Discrete Mathematics and Its Applications*, CRC Press- Taylor and Francis Group, 2013.
- [20] M. Guo, D.V. Dimarogonas, Nonlinear consensus via continuous, sampled, and aperiodic updates, *Int. J. Control* 86 (4) (2013) 567–578, doi:[10.1080/00207179.2012.747735](https://doi.org/10.1080/00207179.2012.747735).
- [21] T. Hayakawa, T. Matsuzawa, S. Hara, Formation control of multi-agent systems with sampled information-relationship between information exchange structure and control performance –, in: *Proceedings of the 45th IEEE Conference on Decision and Control*, 2006, pp. 4333–4338, doi:[10.1109/CDC.2006.377708](https://doi.org/10.1109/CDC.2006.377708).
- [22] H.K. Khalil, *Nonlinear Systems, Third Edition*, Prentice-Hall, Inc., Upper Saddle River, NJ, USA, 2002.
- [23] S. Khoo, L. Xie, Z. Man, Robust finite-time consensus tracking algorithm for multirobot systems, *IEEE/ASME Trans. Mechatron.* 14 (2) (2009) 219–228, doi:[10.1109/TMECH.2009.2014057](https://doi.org/10.1109/TMECH.2009.2014057).
- [24] M. Lemmon, *Event-Triggered Feedback in Control, Estimation, and Optimization*, Springer London, London, pp. 293–358.
- [25] H. Li, X. Liao, T. Huang, W. Zhu, Event-triggering sampling based leader-following consensus in second-order multi-agent systems, *IEEE Trans. Autom. Control* 60 (7) (2015) 1998–2003, doi:[10.1109/TAC.2014.2365073](https://doi.org/10.1109/TAC.2014.2365073).
- [26] Z. Li, Z. Duan, F.L. Lewis, Distributed robust consensus control of multi-agent systems with heterogeneous matching uncertainties, *Automatica* 50 (3) (2014) 883–889, doi:[10.1016/j.automatica.2013.12.008](https://doi.org/10.1016/j.automatica.2013.12.008).
- [27] C.-L. Liu, Y.-P. Tian, Formation control of multi-agent systems with heterogeneous communication delays, *Int. J. Syst. Sci.* 40 (6) (2009) 627–636, doi:[10.1080/00207179.2009.2755762](https://doi.org/10.1080/00207179.2009.2755762).
- [28] N. Liu, R. Ling, Q. Huang, Z. Zhu, Second-order super-twisting sliding mode control for finite-time leader-follower consensus with uncertain nonlinear multiagent systems, *Math. Probl. Eng.* 2015 (2015) 8, doi:[10.1155/2015/292437](https://doi.org/10.1155/2015/292437).
- [29] T. Majumder, R.K. Mishra, A. Sinha, S.S. Singh, P.K. Sahu, Congestion control in cognitive radio networks with event-triggered sliding mode, *AEU - Int. J. Electron. Commun.* 90 (2018) 155–162, doi:[10.1016/j.aue.2018.04.013](https://doi.org/10.1016/j.aue.2018.04.013).
- [30] M. Mazo, P. Tabuada, Decentralized event-triggered control over wireless sensor/actuator networks, *IEEE Trans. Autom. Control* 56 (10) (2011) 2456–2461.
- [31] S. Mondal, R. Su, L. Xie, Heterogeneous consensus of higher-order multi-agent systems with mismatched uncertainties using sliding mode control, *Int. J. Robust Nonlinear Control* 27 (13) (2017) 2303–2320, doi:[10.1002/rnc.3684](https://doi.org/10.1002/rnc.3684).
- [32] A. Msaddek, A. Gaaloul, F. M'sahli, *Output Feedback Robust Exponential Higher Order Sliding Mode Control*, Springer Singapore, Singapore, pp. 53–72.
- [33] R. Olfati-Saber, J.A. Fax, R.M. Murray, Consensus and cooperation in networked multi-agent systems, *Proc. IEEE* 95 (1) (2007) 215–233, doi:[10.1109/JPROC.2006.887293](https://doi.org/10.1109/JPROC.2006.887293).
- [34] E. Peymani, H.F. Grip, A. Saberi, X. Wang, T.I. Fossen, H_∞ almost output synchronization for heterogeneous networks of introspective agents under external disturbances, *Automatica* 50 (4) (2014) 1026–1036, doi:[10.1016/j.automatica.2013.12.021](https://doi.org/10.1016/j.automatica.2013.12.021).
- [35] F. Plestan, V. Brégeault, A. Glumineau, Y. Shtessel, E. Moulay, *Advances in High Order and Adaptive Sliding Mode Control-Theory and Applications*, Springer Berlin Heidelberg, Berlin, Heidelberg, pp. 465–492.
- [36] A.G. Ramm, N.S. Hoang, *Dynamical Systems Method and Applications: Theoretical Developments and Numerical Examples*, Wiley, 2011.
- [37] W. Ren, R.W. Beard, Consensus seeking in multiagent systems under dynamically changing interaction topologies, *IEEE Trans. Autom. Control* 50 (5) (2005) 655–661, doi:[10.1109/TAC.2005.846556](https://doi.org/10.1109/TAC.2005.846556).
- [38] W. Ren, R.W. Beard, E.M. Atkins, Information consensus in multivehicle cooperative control, *IEEE Control Syst.* 27 (2) (2007) 71–82, doi:[10.1109/MCS.2007.338264](https://doi.org/10.1109/MCS.2007.338264).
- [39] C.W. Reynolds, *Flocks, herds and schools: A distributed behavioral model*, in: *SIGGRAPH '87 Proceedings of the 14th annual conference on Computer graphics and interactive techniques*, Anaheim, California, 1987, pp. 25–34.
- [40] M.H. Rezaei, M.B. Menhaj, Stationary average consensus for high-order multi-agent systems, *IET Control Theory Appl.* 11 (5) (2017) 723–731, doi:[10.1049/iet-cta.2016.0129](https://doi.org/10.1049/iet-cta.2016.0129).
- [41] D. Shi, L. Shi, T. Chen, *Event Based State Estimation- A Stochastic Perspective*, Springer, Cham, 2016, doi:[10.1007/978-3-319-26606-0](https://doi.org/10.1007/978-3-319-26606-0).
- [42] A. Sinha, R. Kaur, R. Kumar, A.P. Bhonekar, A cooperative control framework for odour source localisation by multi-agent systems, 2017 <https://hal.archives-ouvertes.fr/hal-01660037>. Working paper or preprint.
- [43] A. Sinha, R. Kumar, R. Kaur, A.P. Bhonekar, Consensus based odour source localisation by multiagent systems, *IEEE Transactions on Cybernetics*, 2018, pp. 1–10, doi:[10.1109/TCYB.2018.2869224](https://doi.org/10.1109/TCYB.2018.2869224).
- [44] A. Sinha, R. Kaur, R. Kumar, A.P. Bhonekar, Cooperative control of multi-agent systems to locate source of an odor, *CoRR* (2017). <http://arxiv.org/abs/1711.03819>.
- [45] A. Sinha, R.K. Mishra, Smooth sliding mode controller design for robotic arm, in: *Proceedings of the 2013 International Conference on Control, Automation, Robotics and Embedded Systems (CARE)*, 2013, pp. 1–5, doi:[10.1109/CARE.2013.6733697](https://doi.org/10.1109/CARE.2013.6733697).
- [46] A. Sinha, R.K. Mishra, Nonlinear autonomous altitude control of a miniature helicopter UAV based on sliding mode methodology, *Int. J. Electron. Commun. Technol.* 6 (1) (2015a), doi:[10.13140/2.1.3983.4569](https://doi.org/10.13140/2.1.3983.4569).
- [47] A. Sinha, R.K. Mishra, Robust altitude tracking of a miniature helicopter UAV based on sliding mode, in: *Proceedings of the 2015 International Conference on Innovations in Information, Embedded and Communication Systems (ICIIECS)*, 2015b, pp. 1–6, doi:[10.1109/ICIIECS.2015.7192889](https://doi.org/10.1109/ICIIECS.2015.7192889).
- [48] A. Sinha, R.K. Mishra, Control of a nonlinear continuous stirred tank reactor via event triggered sliding modes, *Chem. Eng. Sci.* 187 (2018a) 52–59, doi:[10.1016/j.ces.2018.04.057](https://doi.org/10.1016/j.ces.2018.04.057).
- [49] A. Sinha, R.K. Mishra, Temperature regulation in a continuous stirred tank reactor using event triggered sliding mode control, *IFAC-PapersOnLine* 51 (1) (2018b) 401–406, doi:[10.1016/j.ifacol.2018.05.060](https://doi.org/10.1016/j.ifacol.2018.05.060).
- [50] A. Sinha, R.K. Mishra, S. Jaiswal, Robust and smooth nonlinear control of an industrial robot for automated pick and place, in: *Proceedings of the 2015 International Conference on Computing Communication Control and Automation*, 2015a, pp. 1–4, doi:[10.1109/ICCCUEA.2015.11](https://doi.org/10.1109/ICCCUEA.2015.11).
- [51] A. Sinha, P. Prasoon, P.K. Bharadwaj, A.C. Ranasinghe, Nonlinear autonomous control of a two-wheeled inverted pendulum mobile robot based on sliding mode, in: *Proceedings of the 2015 International Conference on Computational Intelligence and Networks*, 2015b, pp. 52–57, doi:[10.1109/CINE.2015.20](https://doi.org/10.1109/CINE.2015.20).
- [52] Y. Su, J. Huang, Stability of a class of linear switching systems with applications to two consensus problems, *IEEE Trans. Autom. Control* 57 (6) (2012) 1420–1430, doi:[10.1109/TAC.2011.2176391](https://doi.org/10.1109/TAC.2011.2176391).
- [53] P. Tabuada, Event-triggered real-time scheduling of stabilizing control tasks, *IEEE Trans. Autom. Control* 52 (9) (2007) 1680–1685.
- [54] P. Tallapragada, N. Chopra, On event triggered tracking for nonlinear systems, *IEEE Trans. Autom. Control* 58 (9) (2013) 2343–2348, doi:[10.1109/TAC.2013.2251794](https://doi.org/10.1109/TAC.2013.2251794).
- [55] V.I. Utkin, *Sliding Modes in Control and Optimization*, Springer, 1992.
- [56] Q. Wang, M. Wu, Y. Huang, L. Wang, Formation control of heterogeneous multi-robot systems, *IFAC Proc. Vol.* 41 (2) (2008) 6596–6601, doi:[10.3182/20080706-5-KR-1001.0112](https://doi.org/10.3182/20080706-5-KR-1001.0112).
- [57] X. Wang, V. Yadav, S.N. Balakrishnan, Cooperative UAV formation flying with obstacle/collision avoidance, *IEEE Trans. Control Syst. Technol.* 15 (4) (2007) 672–679, doi:[10.1109/TCST.2007.899191](https://doi.org/10.1109/TCST.2007.899191).
- [58] Z. Weihua, T.H. Go, Robust decentralized formation flight control, *Int. J. Aerosp. Eng.* 2011 (2011).
- [59] G. Wen, Z. Duan, G. Chen, W. Yu, Consensus tracking of multi-agent systems with Lipschitz-type node dynamics and switching topologies, *IEEE Trans. Circuits Syst. I: Regul. Pap.* 61 (2) (2014) 499–511, doi:[10.1109/TCSI.2013.2268091](https://doi.org/10.1109/TCSI.2013.2268091).
- [60] D. Xue, J. Yao, G. Chen, Y. I. Yu, Formation control of networked multi-agent systems (brief paper), *IET Control Theory Appl.* 4 (10) (2010) 2168–2176, doi:[10.1049/iet-cta.2009.0574](https://doi.org/10.1049/iet-cta.2009.0574).
- [61] Y. Su, J. Huang, Stability of a class of linear switching systems with applications to two consensus problems, in: *Proceedings of the 2011 American Control Conference*, 2011, pp. 1446–1451, doi:[10.1109/ACC.2011.5990782](https://doi.org/10.1109/ACC.2011.5990782).
- [62] X.-G. Yan, S.K. Spurgeon, C. Edwards, *Variable Structure Control of Complex Systems*, Springer, 2017.
- [63] K.D. Young, V.I. Utkin, U. Ozguner, A control engineer's guide to sliding mode control, *IEEE Trans. Control Syst. Technol.* 7 (3) (1999) 328–342.
- [64] W. Yu, G. Chen, M. Cao, Consensus in directed networks of agents with nonlinear dynamics, *IEEE Trans. Autom. Control* 56 (6) (2011a) 1436–1441, doi:[10.1109/TAC.2011.2112477](https://doi.org/10.1109/TAC.2011.2112477).
- [65] W. Yu, G. Chen, W. Ren, J. Kurths, W.X. Zheng, Distributed higher order consensus protocols in multiagent dynamical systems, *IEEE Trans. Circuits Syst. I: Regul. Pap.* 58 (8) (2011b) 1924–1932, doi:[10.1109/TCSI.2011.2106032](https://doi.org/10.1109/TCSI.2011.2106032).
- [66] S.H. Zak, *Systems and Control*, Oxford University Press, 198 Madison Avenue, New York, New York, 10016, 2003.
- [67] Y. Zheng, L. Wang, Distributed consensus of heterogeneous multi-agent systems with fixed and switching topologies, *Int. J. Control* 85 (12) (2012) 1967–1976, doi:[10.1080/00207179.2012.713986](https://doi.org/10.1080/00207179.2012.713986).
- [68] Y. Zheng, Y. Zhu, L. Wang, Consensus of heterogeneous multi-agent systems, *IET Control Theory Appl.* 5 (16) (2011) 1881–1888, doi:[10.1049/iet-cta.2011.0033](https://doi.org/10.1049/iet-cta.2011.0033).
- [69] Y. Zhou, X. Yu, C. Sun, W. Yu, Higher order finite-time consensus protocol for heterogeneous multi-agent systems, *Int. J. Control* 88 (2) (2015) 285–294, doi:[10.1080/00207179.2014.950047](https://doi.org/10.1080/00207179.2014.950047).
- [70] W. Zhu, Z.-P. Jiang, G. Feng, Event-based consensus of multi-agent systems with general linear models, *Automatica* 50 (2) (2014) 552–558, doi:[10.1016/j.automatica.2013.11.023](https://doi.org/10.1016/j.automatica.2013.11.023).